Doctorate of Philosophy

Schrödinger's Catwalk

Brian Flynn

University of Bristol

March, 2021

CONTENTS

LIST OF TABLES

LIST OF FIGURES

LISTINGS

ACRONYMS

C	carbon
^{14}N	nitrogen-14
AI	artificial intelligence
AIC	Akaike information criterion
AICC	Akaike information criterion corrected
BF	Bayes factor
BFEER	Bayes factor enhanced Elo ratings
BIC	Bayesian information criterion
CLE	classical likelihood estimation
CPU	central processing unit
DAG	directed acyclic graph
EDH	experiment design heuristic
ES	exploration strategy
ET	exploration tree
FH	Fermi-Hubbard
FN	false negatives
FP	false positives
GA	genetic algorithm
GES	genetic exploration strategy
GPU	graphics processing unit
HPD	high particle density
IQLE	interactive quantum likelihood estimation
JWT	Jordan Wigner transformation
LE	Loschmidt echo

LTL log total likelihood

ML machine learning

MVEE minimum volume enclosing ellipsoid
MW microwave

NN neural network
NV nitrogen-vacancy
NVC nitrogen-vacancy centre

OF objective function

PBS portable batch system
PGH particle guess heuristic
PL photoluminescence

QC quantum computer
QHL quantum Hamiltonian learning
QL quadratic loss
QLE quantum likelihood estimation
QM quantum mechanics
QML quantum machine learning
QMLA Quantum Model Learning Agent

SMC sequential monte carlo
SVM support vector machine

TLTL total log total likelihood
TN true negatives
TP true positives

VQE variational quantum eigensolver

GLOSSARY

Q	Quantum system which is the target of Quantum Model Learning Agent, i.e. the system to be characterised
champion model	The model deemed by QMLA as the most suitable for describing the target system
chromosome	A single candidate, in the space of valid solutions to the posed problem in a genetic algorithm
expectation value	Average outcome expected by measuring an observable of a quantum system many times, **??**
gene	Individual element within a chromosome
hyperparameter	Variable within an algorithm that determines how the algorithm itself proceeds
instance	A single implementation of the QMLA algorithm, resulting in a nominated champion model
likelihood	Value that represents how likely a hypothesis is. Usually used in the context of likelihood estiamation, **??**
model	The mathematical description of some quantum system, **??**
model space	Abstract space containing all descriptions (within defined constraints such as dimension) of the system as models
probe	Input probe state, $\|\psi\rangle$, which the target system is initialised to, before unitary evolution
results directory	Directory to which the data and analysis for a given run of QMLA are stored
run	Collection of QMLA instances, usually targeting the same system with the same initial conditions

spawn Process by which new models are generated, ususally by combining previously considered models

success rate Fraction of instances within a run where QMLA nominates the true model as champion

term Individual constituent of a model, e.g. a single operator within a sum of operators, which in total describe a Hamiltonian.

volume Volume of a parameter distribution's credible region, **??**

win rate For a given candidate model, the fraction of instances within a run which nominated it as champion

1 MACHINE LEARNING

Machine learning (ML) is the application of statistics, algorithms and computing power to discover meaning and/or devise actions from data. ML has become an umbrella term, encompassing the family of algorithms which aim to leverage computers to learn without being explicitly programmed, as opposed to the more general artificial intelligence (AI), which seeks to make computers behave intelligently, admitting explicit programs to achieve tasks [1]. Its history is therefore imprecise since a number of early, apparently unrelated algorithms were proposed independently, which now constitute ML routines [2, 3]. Nevertheless, the field of ML has been advancing rapidly since the second half of the 20$^{\text{th}}$ century [4], especially recently due to the availability of advanced hardware such as graphics processing units (GPUs), facilitating significant progress through an ever-increasing aresnal of powerful open source software [5, 6, 7].

Throughout this thesis, we endeavour to combine known methods from the ML literature with capabilities of quantum computers (QCs)[1]. Typical ML algorithms, which rely on central processing units (CPUs) or GPUs, are deemed *classical* machine learning, in contrast with quantum machine learning (QML), where QCs are central to processing the data. Similarly to the remit of **??**, here we do not provide an exhaustive account of ML algorithms: rather, we describe only the algorithms which are used in later chapters, referring readers to standard texts for a wider discussion [4, 8].

1.1 CLASSICAL MACHINE LEARNING

Of course the first step in any ML application is to consider the types of available data, with respect to the ensemble of known algorithms. Classical ML is usually described in three categories, broadly based on the format of data on which the insight can be built; we will briefly describe each to provide context to discussions throughout this thesis. Later in this thesis we will use the word *model* for descriptions of quantum systems, but here *model* refers to the mapping between inputs and outputs which the ML algorithm devises.

1.1.1 *Supervised machine learning*

Models are trained using *labelled* data, i.e. each training sample has a known label y_i; or, a set of *feature vectors* $\{\vec{x}_i\}$ are associated with the set of corresponding *classes* $\{y_i\}$ [9]. The output is a predictive tool which aims to reconstruct the classes of unseen feature vectors: in general, we can view the role of ML in this setting as distilling the function f such that

$$f : \vec{x}_i \longmapsto y_i \quad \forall(\vec{x}_i, y_i). \tag{1.1}$$

1 Or simulated QCs, in this thesis.

There are a number of families of algorithms even within the broad category of supervised ML, we define them as

CLASSIFICATION models aim to produce models which can assign unseen instances to the most appropriate label, from a fixed set of available labels [10];

0.1. e.g. labels indicate animals' species, and the feature vector for each sample (data point) encodes the animals' height, weight, number of legs, etc.

REGRESSION models capture the formulaic relationship – which can be either linear or polynamial – between numerical features a the target scalar value, by determining coefficients for each feature. e.g. y is the salary of employees in a company, and the feature vector consists of the individual employees' age, seniority, experience in years, etc.

NEURAL NETWORKS *Universal function approximators*[2]. By invoking a set of linear and non-linear transformations on input data, the *network* is a function of some paramterisation w; neural networks aim to find the optimal network, w', such that Eq. (1.1) is satisfied, $f(w') : \vec{x}_i \longmapsto y_i$.

0.2. Usually used for classification.

0.3. e.g. input *neurons*[3] encode the pixel values of images. The neural network can be used to classify the objects it detects within the image.

SUPPORT VECTOR MACHINE (SVM) Distinguish similar data points by projecitng data into higher dimensional space, and therein finding the hypersurface which separates classes [12].

0.4. Usually used for classification tasks.

0.5. For data $\mathcal{D} \in \mathbb{R}^n$, a hypersurface in $\mathbb{R}^{n-1}$, can be drawn arbitrarilily through the space (e.g. a 2D plane in a 3D space).

0.6. Unseen data can then classified by which partition they are reside in when projected into the n-dimensional space.

0.7. The task of the SVMs is to orient the hypersurface in such a way as to separate distinct classes.

Supervised ML algorithms rely on the existence of a body of labelled samples – the dataset $\mathcal{D}$ – upon which the model can be trained. Training is typically performed on a subset of the data, $\mathcal{D}_t$, usually 80% of samples chosen at random. The remaining (20%) of samples, $\mathcal{D}_v$, are retained for the evaluation of the resultant model: $d \in \mathcal{D}_v$ are not trained upon, so do not contribute to the structure of f as returned by the algorithm. The model therefore can not *overfit*, i.e. simply

2 Including deep learning networks [11].

3 The term *neuron*, also known as *node* or *unit*, derives from the motivation for this class of algorithm: the cells in the brain used for processing information.

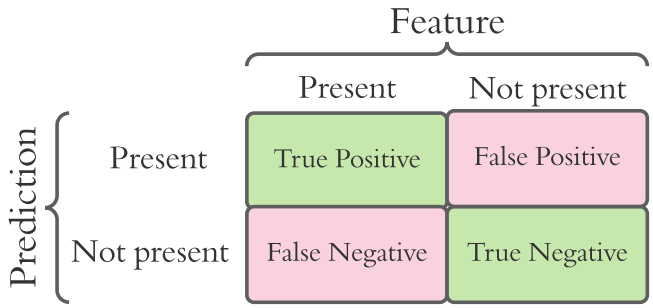

Figure 1.1: Confusion matrix showing the meaning of true positives, true negatives, false positives, false negatives.

recognise particular samples and label them correctly, without any meaningful inference. The evalutation thus captures how the model can be expected to perform on future, unlabelled data.

1.1.2 *Performance metrics*

An important step is the fair assessment of algorithms, then, which is achieved through a number of *performance metrics*. In each supervised ML, the machine attempts to learn the structure of f that optimises some internal objective function (OF), e.g. minimising the average distance between predicted and target labels for regression, $\sum_{d \in \mathcal{D}_t} y_d - y'_d$. To assess the resultant model, we introduce a number of *performance metrics*, which aim to measure serveral perspectives of the model's efficacy, by considering the model's predictions with respect to $\mathcal{D}_v$.

By definition of the data format, it is relatively straightforward to define metrics for supervised routines: the classes assigned to feature vectors, y'_i, can be quantitatively assessed with respect to their true class, y_i. For example, in *binary classification*, the output of the model is either correct or incorrect, allowing us to meaningfully assess its average performance. Likewise, for numerical targets, the difference $\left|y_i - y'_i\right|$ between the output, y'_i, and the target, y_i for each sample cumulatively indicate the strength of the model.

There are a large number of quantities and performance metrics against which to judge models' outputs. In binary classification, we care about whether the model predicts that a given feature is present, and whether it predicts features incorrectly. For example, the model aims to classify whether or not a dog is present in an image. These type of binary predictions have four outcomes, which can be summarised in a *confusion matrix* (Fig. 1.1), defined as in Table 1.1.

	y has feature	y' has feature
True positives (TP)	✓	✓
False positives (FP)	×	✓
True negatives (TN)	×	×
False negatives (FN)	✓	×

Table 1.1: Classification metrics. We define classification outcomes based on whether the considered feature was present and/or predicted.

We can use the concepts of Table 1.1 to define a series of *rates* which characterise the model's predictions.

ACCURACY The overall rate at which the algorithm predicts the correct result.

$$\frac{TP + TN}{TP + TN + FN + FP} \tag{1.2a}$$

PRECISION Positive predicitve rate. Of those *predicted to have* the feature of interest, what percentage *actually have* the feature.

$$\frac{TP}{TP + FP} \tag{1.2b}$$

SENSITIVITY True positive rate (also known as *recall*). Of those which *actually have* the feature, what percentage are *predicted to have* the feature.

$$\frac{TP}{TP + FN} \tag{1.2c}$$

SPECIFICITY True negative rate. Of those which *do not actually have* the feature of interest, how many are *predicted not to* have the feature.

$$\frac{TN}{TN + FP} \tag{1.2d}$$

Each metric has clear advantages, but consider also their drawbacks:
1. Accuracy can be extremely misleading. for example, in a dataset with only 100 instances of the feature of interest, a model predicting 9,900 true negatives and 1,100 false negatives will give 99% accuracy, despite not having found a single positive sample. This is clearly of no use in identifying the minority of cases which are of actual interest.
2. Sensitivity can be inflated by over-fitting to positive cases. That is, by predicting the feature as present in all cases, all true instances of the feature will be found, however all false instances

True positives	False negatives	False positives	Precision	Sensitivity	F_1-score
500	500	1000	33	50	$(\frac{2\times33\times50}{33+50}) = 37$
500	500	500	50	50	$(\frac{2\times50\times50}{50+50}) = 50$
1000	0	1000	50	100	$(\frac{2\times50\times100}{50+100}) = 67$
1000	0	0	100	100	$(\frac{2\times100\times100}{100+100}) = 100$

Table 1.2: F_1-score examples.

will be labelled as having the feature, so the model has not helped separate the data. The model willl yield a high rate of true positives (TP) but also a high rate of false positives (FP).
3. Precision can be high for extremely selective models, i.e. those which are conservative in predicting the presence of the feature. By predicting relatively few positive instances, it can ensure that a high proportion of its predictions are correct. The absolute number of instances identified, however, is relatively low, as a proportion of the total number in the dataset.
4. Specificity, similar to sensitivity, can easily mislead by identifying very few instances as having the target feature. Then, it will correctly predict most non-present instances as false, but will not identify the few instance of interest.

Clearly, the performance metric must be chosen with due consideration for the application; e.g. in testing for a medical condition, rather than incorrectly telling a patient they do not have the condition because the model predicted they were feature-negative, it is preferable to incorrectly identify some patients as feature-positive (since they can be retested). In this case, high accuracy is crucial, at the expense of precision. It is clearly appropriate to blend together the usual metrics, in order to derive performance metrics which balance the priorities of the outcomes. In general – including in this thesis – the most important aspects of a ML are precision and sensitivity: a model which performs well with respect to *both* of these is sensitive to the feature, but precise in its predictions. A quantity which captures both of these is the F_β-score,

$$f_\beta = \left(1+\beta^2\right) \frac{\text{precision} \times \text{sensitivity}}{(\beta^2 \times \text{precision}) + \text{sensitivity}}, \tag{1.3}$$

where $\beta \in \mathbb{R}$ is the relative weight of importance between sensitivity and precision. In particular, considering precision and sensitivity as equally important, i.e. $\beta = 1$, we have the F_1-score,

$$f_1 = \frac{2 \times \text{precision} \times \text{sensitivity}}{\text{precision} + \text{sensitivity}}. \tag{1.4}$$

For examples of how F_1-score balances these considerations, see Table 1.2.

1.1.3 *Unsupervised machine learning*

Contrary to supervised algorithms, unsupervised methods operate on *unlabelled* data, $\mathcal{D}$. This is often summarised as finding structure within unstructured data. Again, we can further compartmentalise methods under this umbrella [13]. Although we do not utilise these methods in this thesis, we briefly summarise them here for completeness.

CLUSTERING Finding datapoints which are similar to each other, according to some distance metric.

4.1. e.g. online retailers grouping together customers with similar preferences, in order to tailor advertising campaigns.

DIMENSIONALITY REDUCTION Reducing the feature vector of each sample in a dataset to essential components, which may be amalgamations of original features, while retaining structure within the data.

4.2. this can be used for visualisation to allow for inspection of complex datasets, e.g. plotting users of a social network as nodes on a 2D map, where distinct social groups are kept distant.

ASSOCIATION LEARNING Discover correlations among data.

4.3. For instance, a supermarket may find that purchasers of certain products are likely also to buy others, providing actionable insight e.g. purchases involving bread also include butter in 50% of cases, so positioning these nearby may increase sales by reminding consumers of their compatibility.

SEMI-SUPERVISED LEARNING Combine elements of supervised and unsupervised algorithms, to achieve a task beyond the remit of either alone. This often means classifying data where only occur a small subset of the total dataset is labelled.

4.4. e.g. in facial recognition, a clustering algorithm finds similarities between individual people in photos, and identifies a single person present across a number of photos, and associates those photos together. It combines this with a small set of photos for which people have been tagged, locates the same person and automatically tags them in the wider set of photos.

1.1.4 *Reinforcement learning*

A third category of ML algorithms are reinforcement learning (RL). These are methods where an *agent* interacts with some environment, and refines a *policy* for reacting to different stimuli. As such, the agent can, in principle, deal with a wide array of situations. These methods underly technologies such as self-driving cars, which inspect their surroundings through *sensors*;

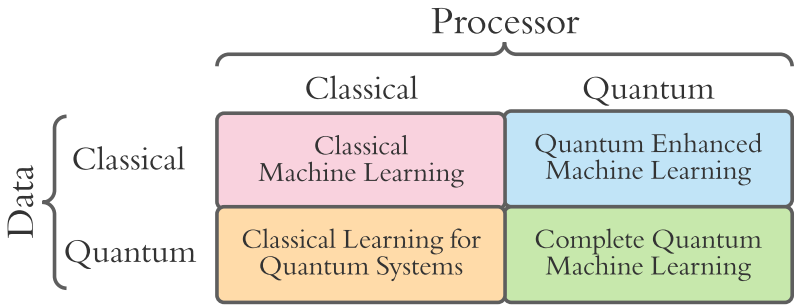

Figure 1.2: Types of quantum machine learning.

compute an *action* according to the policy; implement that action through *actuators*. Following an action, the agent senses whether that action was beneficial or detrimental, and receives a *reward* or *punishment* accordingly. Highly rewarded actions are likely to be repeated in future, allowing the agent to learn what response is appropriate to situational parameters, e.g. a self-driving car braking at a red light is rewarded, while braking at a green light is punished.

The concept of a machine's *agency* is an ongoing discussion in the ML community [14, 15], and is important in this thesis also, when we define our model learning protocol as an agent, since it designs models by interacting with the envinroment of the target quantum systems. We will revisit the concept in **??**.

1.2 QUANTUM MACHINE LEARNING

A growing domain is the development of ML algorithms which run on quantum hardware, or exploit data from quantum systems; generally referred to as QML [16, 17]. There are a number of metehodologies which are referred to as QML; for clarity, we define the main branches here, as shown in Fig. 1.2.

CLASSICAL MACHINE LEARNING refers to standard ML as described in Section 1.1, i.e. where the processors are CPUs or GPUs, and the applications are not of specific interest to problems in the quantum domain. Recently, this branch has encompassed quantum *inspired* ML, which still target classical problems, but use subroutines which were orginally found in the context of QML [18].

QUANTUM ENHANCED MACHINE LEARNING A quantum co-processor is leveraged on classical data for some provable speedup, i.e. data that could otherwise be processed purely classically, is encoded, loaded onto and processed by quantum hardware. The quantum counterparts of classical ML algorithms aim to solve the same problems, e.g. as neural networks (NNs) [19, 20] and principle component analysis [21].

classical learning for quantum systems Classical processors are employed to extract insight on problems arising from quantum systems, e.g. data is taken from a quantum system and analysed via purely classical methods. For instance, methods which aim to represent quantum states efficiently by leveraging NNs [22, 23].

complete quantum machine learning Data of a quantum nature is processed – at least partially – by quantum processors. The most common technique here is variational quantum eigensolver (VQE), which simulates quanutm systems on QCs, in order to retrieve quantum systems' ground states [24]. The algorithm relies on a classical optimisation routine, but was devised explicitly for implementation on quantum hardware.

The algorithms described in **??** and the applications in **??**–**??** can be described as classical learning for quantum systems. This is because the data upon which the applications are built represent quantum systems, but are processed through classical ML algorithms in order to derive insight about those systems. We caveat that it is feasible, and indeed the long term intention of such algorithms, to run in conjunction with a quantum co-processor, which would represent and evolve quantum systems, but all processing presented here are through strictly classical architecture.

1.3 Genetic algorithms

In later chapters we will use a class of optimisation techniques known as *evolutionary algorithms* [25, 26]. In particular, *genetic algorithms (GAs)* are central to our primary applications, specifically in Chapter 2. Here we describe genetic algorithms (GAs) in general terms for reference in later chapters.

GAs work by assuming a given problem can be optimised, if not solved, by a single candidate among a fixed, closed space of candidates, called the population, $\mathcal{P}$. A number of candidates are sampled at random from $\mathcal{P}$ into a single *generation*, and evaluated through some objective function (OF), which assesses the fitness of the candidates at solving the problem of interest. Candidates from the generation are then mixed together to produce the next generation's candidates: this *crossover* process aims to combine only relatively strong candidates, such that the average candidates' fitness improve at each successive generation, mimicing the biological mechanism whereby the genetic makeup of offspring is an even mixture of both parents through the philosophy of *survival of the fittest*. The selection of strong candidates as parents for future generations is therefore imperative; in general parents are chosen according to their fitness as determined by the OF. Buidling on this biological motivation, much of the power of GAs comes from the concept of *mutation*: while offspring retain most of the genetic expressions of their parents, some elements are mutated at random. Mutation is crucial in avoiding local optima of the OF landscape by maintaining diversity in the examined subspace of the population.

GAs are not defined either as supervised or unspervised methods; this designation depends on the OF. If candidates are evaluated with respect to labelled data, we can consider that GA

supervised, otherwise unsupervised. Pseudocode for a generic GA is given in Algorithm 1, but we can also informally define the procedure as follows. Given access to the population, $\mathcal{P}$,

1. Sample N_m candidates from the population at random
   (a) call this group of candidates the first generation, μ.
2. Evaluate each candidate $\gamma_j \in \mu$
   (a) each γ_j is assigned a fitness, g_j;
   (b) the fitness is computed through an objective function acting on the candidate, i.e. $g_j = g(\gamma_j)$.
3. Map the fitnesses of each candidate, $\{g_j\}$, to selection probabilities for each candidate, $\{s_j\}$
   (a) e.g. by normalising the fitnesses, or by removing some poorly-performing candidates and then normalising.
4. Generate the next generation of candidates
   (a) Reset $\mu = \{\}$;
   (b) Select pairs of parents, $\{\gamma_{p_1}, \gamma_{p_2}\}$, from μ
      i. Each candidate's probability of being chosen is given by their s_j.
   (c) Cross over $\{\gamma_{p_1}, \gamma_{p_2}\}$ to produce children candidates, $\{\gamma_{c_1}, \gamma_{c_2}\}$
      i. mutate $\gamma_{c_1}, \gamma_{c_2}$ according to some random probabilistic process;
      ii. keep γ_{c_i} only if it is not already in μ, to ensure N_m unique candidates are tested at each generation.
   (d) until $|\mu| = N_m$, iterate to step (b).
5. Until the N_g^{th} generation is reached, iterate to step 2.;
6. The strongest candidate on the final generation is deemed the solution to the posed problem.

Candidates are manifested as *chromosomes*, i.e. strings of fixed length, whose entries, called *genes*, each represent some element of the system. In general, genes can have continuous values, although usually, and for all purposes in this thesis, genes are binary, capturing simply whether or not the gene's corresponding feature is present in the chromosome.

1.3.1 *Example: knapsack problem*

One commonly referenced combinatorial optimisation problem is the *knacksack problem*: given a set of objects, where each object has a defined mass and also a defined value, determine the set of objects to pack in a knapsack which can support a limited weight, such that the value of the packed objects is maximised. Say there are n objects, we can write the vector containing the values of those objects as $\vec{v}$, and the vector of their weights as $\vec{w}$. We can then represent

Algorithm 1: Genetic algorithm

Input: $\mathcal{P}$ // Population of candidate models
Input: $g()$ // objective funtion
Input: map_g_to_s() // function to map fitness to selection probability
Input: select_parents() // function to select parents among generation
Input: crossover() // function to cross over two parents to produce offspring
Input: N_g // number of generations
Input: N_m // number of candidates per generation

Output: γ' // strongest candidate

$\mu \leftarrow \text{sample}\,(\mathcal{P}, N_m)$
for $i \in 1, ..., N_g$ **do**
  for $\gamma_j \in \mu$ **do**
    $g_j \leftarrow g(\gamma_j)$ // assess fitness of candidate
  end
  $\{s_j\} \leftarrow$ map_g_to_s($\{g_j\}$) // map fitnesses to normalised selection probability
  $\mu_c = \arg\max_{s_j}\{\gamma_j\}$ // record champion of this generation

  $\mu \leftarrow \{\}$ // empty set for next generation
  while $|\mu| < N_m$ **do**
    $p_1, p_2 \leftarrow$ select_parents($\{s_j\}$) // choose parents based on candidates' s_j
    $c_1, c_2 \leftarrow$ crossover(p_1, p_2) // generate offspring candidates based on parents
    for $c \in \{c_1, c_2\}$ **do**
      if $c \notin \mu$ **then**
        $\mu \leftarrow \mu \cup \{c\}$ // keep if child is new
      end
    end
  end
end
$\gamma' \leftarrow \arg\max_{s_j}\{\gamma_j \in \mu\}$ // strongest candidate on final generation

return γ'

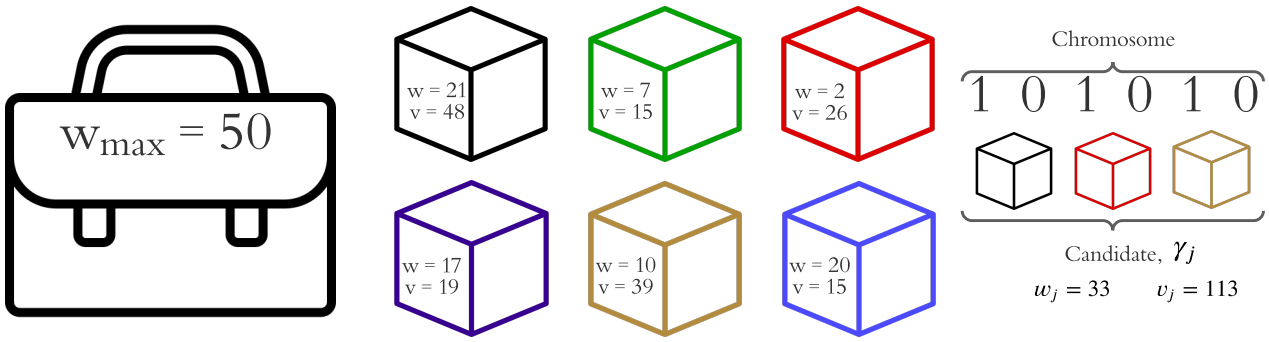

Figure 1.3: Depiction of the knapsack problem. **Left**, A knapsack which can hold any number of objects but is constrained by the total weight it can support, $w_{max} = 50$. **Centre**, A set of objects are available, each with associated weight, w, and value v. The objective is to find the subset of objects which maximise the total value, while not exceeding the capacity of the knapsack. **Right**, An example chromosome, i.e. candidate γ_j, where the bits of the chromosome indicate whether the corresponding object is included, allowing for calculation of the total weight and value of the candidate, w_j, v_j.

configurations of object sets as candidate vectors $\vec{\gamma}_j$, whose genes are binary, and simply indicate whether or not the associated object is included in the set. For example, with $n = 6$,

$$\gamma_j = 100001 \implies \vec{\gamma}_j = (1 \quad 0 \quad 0 \quad 0 \quad 0 \quad 1), \tag{1.5}$$

indicates a set of objects consisting only of those indexed first and last, with none of the intermediate objects included.

The fitness of any candidate is then given by the total value of that configuration of objects, $v_j = \vec{v} \cdot \vec{\gamma}_j$, but candidates are only admitted[4] if the weight of the corresponding set of objects is less than the capacity of the knapsack, i.e. $\vec{w}_j \cdot \vec{\gamma}_j \leq w_{max}$.

For example where each individual object has value < 50 and weight < 25 and $w_{max} = 50$, recalling $\gamma_j = 100001$, say,

$$\vec{v} = (48 \quad 15 \quad 26 \quad 19 \quad 39 \quad 15) \implies v_j = \vec{\gamma}_j \cdot \vec{v} = 48 + 15 = 63; \tag{1.6a}$$

$$\vec{w} = (21 \quad 7 \quad 2 \quad 17 \quad 10 \quad 20) \implies w_j = \vec{\gamma}_j \cdot \vec{w} = 21 + 20 = 41. \tag{1.6b}$$

We can hence assess the fitness of γ_j as 63 and deem it a valid candidate since it does not exceed the weight threshold. We can likewise compute the total weight and value of a series

4 Note there are alternative strategies to dealing with candidates who violate the weight condition, such as to impose a penalty within the OF, but for our purposes let us assume we simply disregard violators.

of randomly generated candidates, and deem them valid or not. Table 1.3 shows a set of 12 randomly generated candidates, of which ten are valid.

Name	Candidate	Value	Weight	Valid
γ_1	110011	117	58	No
γ_2	101010	113	33	Yes
γ_3	011110	99	36	Yes
γ_4	011011	95	39	Yes
γ_5	111000	89	30	Yes
γ_6	010111	88	54	No
γ_7	100010	87	31	Yes
γ_8	110001	78	48	Yes
γ_9	011101	75	46	Yes
γ_{10}	110000	63	28	Yes
γ_{11}	000011	54	30	Yes
γ_{12}	000101	34	37	Yes

Table 1.3: Candidate solutions to the knapsack problem for randomly generated chromosomes.

The strongest (valid) candidates from Table 1.3 are $101010, 011110$. By spawning from these candidates through a one-point crossover at the midpoint[5], we get $\gamma_{c_1} = 101110, \gamma_{c_2} = 011010$, from which we can see $v_{c_1} = 132, w_{c_1} = 50$, i.e. by combining two strong candidates we produce the strongest-yet-seen valid candidate.

By repeating this procedure, it is expected to uncover candidates which optimise v_j while maintining $w_j \leq w_{max}$, or at least to produce near-optimal solutions, using far less time/resources than brute-force evaluation of all candidates, which is usually sufficient. For instance, with $n = 100$ objects to consider, there are $2^{100} \approx 10^{30}$ candidates to consider; the most powerful supercomputers in the world currently claim on the order of Exa-FLOPs, i.e. 10^{18} operations per second, of which say $\mathcal{O}(1000)$ operations are required to test each candidate, meaning 10^{15} candidates can be checked per second in a generous example. This would still require 10^{12} seconds to solve absolutely, so it is reasonable in cases like this to accept *approximately optimal* solutions[6].

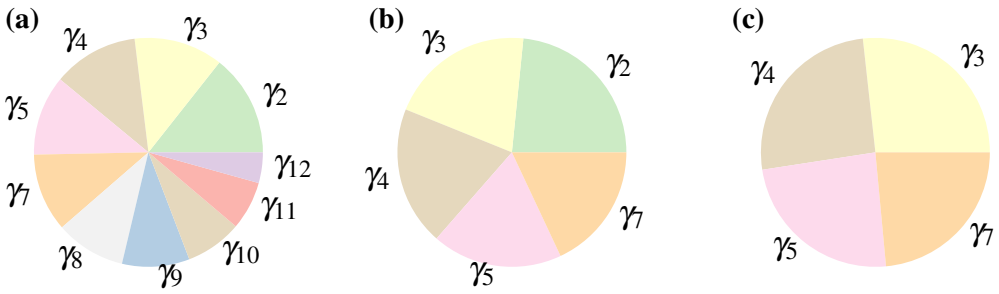

Figure 1.4: Roulette wheels showing selection probability s_i for corresponding candidates γ_i. Colours here only distinguish candidates, they do not encode any information. **b**, The set of potential parents is truncated to include only the strongest five candidates. **a**, All valid candidates are assigned selection probability based on their value in Table 1.3. **c**, After one parent (γ_2) has been chosen, it is removed from the roulette wheel and the remaining candidates' probabilities are renormalised for the selection of the second parent.

1.3.2 *Selection mechanism*

A key subroutine of every GA is the mechanism through which it nominates candidates from generation μ as parents to offsping candidates in $\mu + 1$ [27]. All mechanisms have in common that they act on a set of candidates from the previous generation, where each candidate, γ_j, has been evaluated and has fitness value, g_j. Among the viable schemes for selecting individual parents from the set of candidates, μ are

- Rank selection: candidates are selected with probabilty proportional to their ranking relative to the fitness of contemporary candidates in the same generation;
- Tournament selection: a subset of k candidates are chosen at random from μ, of which the candidate with the highest fitness is taken as the parent;
- Stochastic universal sampling: candidates are sampled proportional to their fitness, but the sampling algorithm is biased to ensure high-fitness candidates are chosen at least once within the generation.

We will only detail the mechanism used in later applications within this thesis: fitness proportional selection, known as *roulette selection* [27]. This is a straightforward strategy where we directly map candidates' fitness, g_i to a selection probability, s_i, simply by normalising $\{g_i\}$, allowing us to visualise a roulette wheel of uneven wedges, each of which correspond to a candidate. Then we need only conceptually spin the roulette wheel to select the first parent, γ_{p_1}.

5 One-point crossovers are detailed in Section 1.3.3 with this example shown in Fig. 1.5.
6 Simply put: in machine learning, *good enough* is good enough. We will adopt this philosophy for the remainder of this thesis and life.

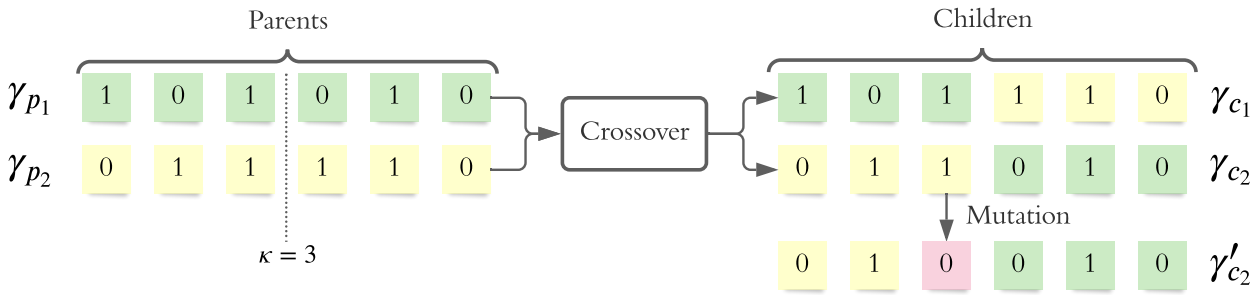

Figure 1.5: Crossover and mutation of chromosomes. Two parents, $\{\gamma_{p_1}, \gamma_{p_2}\}$, are nominated from the process in Fig. 1.4. They are then crossed-over via a one-point crossover with crossing point $\kappa = 3$, resulting in children candidates $\{\gamma_{c_1}, \gamma_{c_2}\}$. One child chromosome is mutated to yield a new candidate, γ'_{c_2}. The candidates added to the next generation are then $\{\gamma_{c_1}, \gamma'_{c_2}\}$.

We then remove γ_{p_1} from the set of potential parents, renormalise the remaining $\{s_i\}$, and spin the wheel again to choose the second parent, γ_{p_2}. The roulette selection is shown in Fig. 1.4.

Practically, we repeat the process outlined until the next generation is filled, usually we have $|\mu| = N_m$, and desire that every generation should contain the same N_m candidates, so we repeat the roulette selection $N_m/2$ times per generation, since every pair of parents yield two offspring. It is important that meaningful differences in fitness are reflected by the selection probability, which is difficult to ensure for large N_m, e.g. with ten models, the strongest candidate is only a marginally more probable parent than the worst – this effect is amplified for larger N_m. We therefore wish to reduce the set of potential parents to ensure high quality offspring: we truncate μ and retain only the highest-fitness $\frac{N_m}{2}$ models as selectable parents.

1.3.3 *Reproduction*

When a pair of parents have been nominated by the selection mechanism above, it remains to use those parents to *reproduce*, i.e. to produce offspring which should inherit and improve upon the properties of their parents. Here we use a *one point crossover*, whereby the two parent chromosomes are mixed together to form two offspring, about a single point, κ: for candidates of n genes, the first κ genes of γ_{p_1} are conjoined with the latter $n - \kappa$ genes of γ_{p_2}. Often κ is restricted to the midpoint of the chromosomes, although in general we need not impose this: we will instead consider $\kappa \in \left(\frac{n}{4}, \frac{3n}{4}\right)$, e.g. with $n = 12$, $\kappa \in (3, 9)$. The one-point crossover is shown for $n = 6$ with $\kappa = 3$ in Fig. 1.5, recalling the chromosome structure from Section 1.3.1.

By allowing κ other than the midpoint, we drastically increase the number of combinations of parents available for reproduction. Finally, then, parent selection is done by constructing a database of pairs of potentital parents with all available crossover points, with selection

probability given by the product of their individual fitnesses. This is conceptually equivalent to selection via roulette wheel as above. Recalling the fitnesses (values) of Table 1.3, we generate the parent selection database:

Parent 1	Parent 2	κ	s_{ij}
γ_2	γ_3	2	$11,187\ (= 113 \times 99)$
γ_2	γ_3	3	$11,187$
γ_2	γ_3	4	$11,187$
γ_2	γ_4	2	$10,735\ (= 113 \times 95)$
γ_2	γ_4	3	$10,735$
γ_2	γ_4	4	$10,735$
		$\vdots$	
γ_5	γ_7	2	$7,743\ (= 89 \times 87)$
γ_5	γ_7	3	$7,743$
γ_5	γ_7	4	$7,743$

Table 1.4: Example of parent selection database. Pairs of parents are selected together, with the (unnormalised) selection probability, s_{ij}, given by the product of the individual candidates' fitnesses. Pairs of parents are repeated in the database for differing κ, and all κ are equally likely.

The GA maintains diversity in the subspace of $\mathcal{P}$ it studies, by *mutating* some of the newly proposed offspring candidates. Again, there are a multitude of approaches for this step [28], but for brevity we only describe those used in this thesis. For each proposed child candidate, γ_c, we probabilistically mutate each gene with some mutation rate r_m: if a mutation occurs, the child is replaced by γ_c'. That is, γ_c' is added to the next generation, and γ_c is discarded. r_m is a *hyperparameter* of the GA: the performance of the algorithm can be optimised by finding the best r_m for a given problem.

1.3.4 *Candidate evaluation*

Within every generation of the GA, each candidate must be evaluated, so that the relative strength of candidates can be exploited in constructing candidates for the next generation. In the example of the knapsack problem used above, candidates were evaluated by the value of their contents, but also by whether they would fit in the knapsack. Idenitfiyng the appropriate method by which to evaluate candidates is arguably the most important aspect of designing a GA: while the choice of hyperperameters (N_g, N_m, r_m) dictate the efficacy of the search, the lack of an effective metric by which to distinguish candidates would render the procedure pointless. Considerations are hence usually built into the objective function (OF); GAs implementations later in this thesis therefore demand we design OFs with respect to the individual application.

2

GENETIC ALGORITHMS

The Quantum Model Learning Agent (QMLA) framework lends itself easily to the family of optimsation techniques called *evolutionary algorithms*, where individuals, sampled from a population of candidates, are considered as solutions to the given problem. Candidates are batched in *generations*, such that iterative generations aim to efficiently search the available population by mimicing biological evolutionary mechanisms [25]. In particular, we develop an exploration strategy (ES) which incorporates a genetic algorithm (GA) in the construction of models; GAs are a subset of evolutionary algorithms where candidate solutions are expressed as strings of numbers representing some configuration of the system of interest [29]. We describe the concepts of GAs in Section 1.3, so we begin this chapter by describing the adaptations which allow us to build a genetic exploration strategy (GES) within QMLA.

2.1 ADAPTATION TO QMLA FRAMEWORK

Unlike the generic aspects of GAs described in Section 1.3, in the context of QMLA, we must deviate from default mechanisms. The overarching goal of QMLA – to characterise some black box quantum system, Q – proceeds by designing and performing experiments upon Q which enable us to improve the modelling of $\hat{H}_0$. Nothing described so far provides a natural objective function (OF), upon which GAs rely to assess the suitability of candidates relative to contemporaries. We can not assume knowledge of $\hat{H}_0$ while generating candidates models, so we can not simply invoke some loss function with respect to the target model, for example. Instead, we must devise schemes which exploit the knowledge we *do* have about each candidate $\hat{H}_j$, which is the primary challenge in building an ES based on a GA. We propose and discuss a number of options in Section 2.2.

Common to all proposed OFs, however, is that candidates should first be trained before evaluation, so that their assessment is based on their actual power in describing Q, rather than some initial paramterisation which may not capture their potential. This is a tenet of QMLA: for each candidate $\hat{H}_j(\vec{\alpha}_j)$, we use a subroutine to optimise $\vec{\alpha}_j$; as in earlier applications of QMLA, for this study we rely on quantum Hamiltonian learning (QHL) as the parameter optimisation subroutine.

Ultimately, the conceived role of a GA within QMLA is to generate the sets of models to place on successive branches[1] of an exploration tree (ET) as depicted in **??**. The apparatus within QMLA which facilitates novel model generation techniques is the exploration strategy (ES). Here we will design an ES which acts in cooperation with a GA: the ES specifies that consolidation of a generation μ involve evaluating the *fitness*, g_i, of each candidate, $\hat{H}_i$, via the chosen OF; the

1 Branches in QMLA and generations of the genetic algorithm are equivalent here.

GA then maps $\{g_i\}$ of each $\hat{H}_i \in \mu$ to a selection probability, and composes new candidates via crossover, Section 1.3.3. Recall from **??**, that we capture the space of available terms as $\mathcal{T}$, i.e. we list – in advance – the feasible terms which may be included in candidate models[2], with $N_t = |\mathcal{T}|$ the number of terms considered. QMLA is then an optimisation algorithm, attempting to find the set $\mathcal{T}'$ which *best* represents the true terms $\mathcal{T}_0$. Note, this does not require idenitifcation of the precise true model to be successful, as insight can be gained from approximate models which capture the physics of the target system. We introduce metrics for success in Section 2.1.2. We recognise the limitations this structure imposes: we can only identify terms which were conceived in advance; this may restrict QMLA's applicability to entirely unknown systems, where such a primitive set can not even be compiled.

The structure of the overall QMLA algorithm (recall **??**) is unchanged. In a GES:

- Branches: models are still grouped in branches, here called generations;
- Training: models are still trained, again through QHL;
- Consolidation: all models are evaluated according the the OF to be described in Section 2.2, so branches are consolidated by ranking models according to their fitness;
- Spawning: new models are spawned through the GA by selecting pairs of parents for crossover, with the resultant offspring models probabilistically mutated.

The design of any ES centres on the implementation of the generate_models subroutine – we summarise the GES's method in Algorithm 2. We can restate the informal description of GAs[3], now in the context of QMLA, as

1. Sample N_m models from $\mathcal{P}$ at random
   (a) this is the first generation, μ.
2. Evaluate each model $\hat{H}_j \in \mu$
   (a) train $\hat{H}_j$ through QHL;
   (b) apply the objective function to assign the model's fitness, g_j.
3. Map the fitnesses of each model, $\{g_j\}$, to selection probabilities for each model, $\{s_j\}$
   (a) e.g. by normalising the fitnesses, or by removing some poorly-performing models and then normalising.
4. Generate the next generation of models
   (a) Reset $\mu = \{\}$;
   (b) Select pairs of parents, $\hat{H}_{p_1}, \hat{H}_{p_2}$, from μ
      i. Each model's probability of being chosen is proportional to their s_j;
   (c) Cross over $\hat{H}_{p_1}, \hat{H}_{p_2}$ to produce children models, $\hat{H}_{c_1}, \hat{H}_{c_2}$
      i. mutate $\hat{H}_{c_1}, \hat{H}_{c_2}$ according to some random probabilistic process;

2 Recall that models impose structure on sets of terms: $\hat{H}_j = \vec{\alpha}_j \cdot \vec{T}_j = \sum_{k \in \{j\}} \alpha_k \hat{t}_k$.

3 First stated on Page 9.

ii. $\mu \leftarrow \mu \cup \{\hat{H}_{c_i}\}$, only if $\hat{H}_{c_i}$ is not already in μ, to ensure N_m unique models are tested at each generation;

(d) until $|\mu| = N_m$, iterate to step (b).

5. Until the N_g^{th} generation is reached, iterate to step 2..
6. The strongest model on the final generation is deemed the approximation to the system, $\hat{H}'$.

2.1.1 *Models as chromosomes*

We first need a mapping from models to chromosomes; this is straightforward given the description of chromosomes as binary strings, exemplified in Section 1.3.1. We assign a gene to every term in $\mathcal{T}$, so that candidate models are succinctly represented by bit strings of length N_t. We give an example of the mapping between models and chromosomes in Table 2.1. Given that every model is contained in the space of bit strings spanned by N_t bits, we can say that there are a total of 2^{N_t} available models in the model space.

2.1.2 *F_1-score*

We need a metric against which to evaluate models, and indeed the entire QMLA procedure. We can gauge the performance of QMLA's model search by the quality of candidate models produced at each generation, so we introduce a metric to act as proxy for model quality: the F_1-score, denoted f. We define F_1-score formally in this section, but in short, $f \in (0, 1)$ indicates the degree to which $\hat{H}_i$ captures the physics of the target system: $f = 0$ indicates that $\hat{H}_i$ shares no terms with $\hat{H}_0$, while $f = 1$ is found uniquely for $\hat{H}_i = \hat{H}_0$. We defined F_1-score, as well as a number of metrics in the field of classification in machine learning (ML), in Section 1.1.2; here we modify those definitions to align with the nomenclature of QMLA.

We emphasise that the goal of this work is to identify the *model* which best describes quantum systems, and not to improve on parameter-learning when given access to particular models, since those already exist to a high standard [30, 31]. Therefore we can consider QMLA as a classification algorithm, with the goal of classifying whether individual terms $\hat{t}$ from a set of available terms $\mathcal{T} = \{\hat{t}\}$ are helpful in describing data which is generated by $\hat{H}_0$, whose terms constitute $\mathcal{T}_0$. Candidate models $\hat{H}_i$ then have $\mathcal{T}_i$. We can assess $\hat{H}_i$ using standard metrics used regularly in the ML literature, which simply count the number of terms identified correctly and incorrectly:

- true positives (TP): number of terms in $\mathcal{T}_0$ which are in $\mathcal{T}_i$
- true negatives (TN): number of terms not in $\mathcal{T}_0$ which are also not in $\mathcal{T}_i$
- false positives (FP): number of terms in $\mathcal{T}_i$ which are not in $\mathcal{T}_0$
- false negatives (FN): number of terms in $\mathcal{T}_0$ which are not in $\mathcal{T}_i$.

Model		Chromosome					
	$\vec{T}$	$\hat{\sigma}^x_{(1,2)}$	$\hat{\sigma}^z_{(1,2)}$	$\hat{\sigma}^y_{(2,3)}$	$\hat{\sigma}^x_{(2,3)}$	$\hat{\sigma}^y_{(2,3)}$	$\hat{\sigma}^x_{(2,3)}$
γ_{p_1}	$(\hat{\sigma}^x_{(1,2)} \quad \hat{\sigma}^z_{(1,2)} \quad \hat{\sigma}^y_{(2,3)})$	1	0	1	0	1	0
γ_{p_2}	$(\hat{\sigma}^z_{(1,2)} \quad \hat{\sigma}^y_{(2,3)} \quad \hat{\sigma}^z_{(2,3)})$	0	0	1	0	1	1
γ_{c_1}	$(\hat{\sigma}^x_{(1,2)} \quad \hat{\sigma}^z_{(1,2)} \quad \hat{\sigma}^y_{(2,3)} \quad \hat{\sigma}^z_{(2,3)})$	1	0	1	0	1	1
γ_{c_2}	$(\hat{\sigma}^z_{(1,2)} \quad \hat{\sigma}^y_{(2,3)})$	0	0	1	0	1	0
γ'_{c_2}	$(\hat{\sigma}^z_{(1,2)} \quad \hat{\sigma}^x_{(2,3)} \quad \hat{\sigma}^y_{(2,3)})$	0	0	1	1	1	0

Table 2.1: Mapping between QMLA's models and chromosomes used by a genetic algorithm. Example shown for a three-qubit system with six possible terms, $\hat{\sigma}^w_{i,j} = \hat{\sigma}^w_i \hat{\sigma}^w_j$. Model terms are mapped to binary genes: if the gene registers 1 (0) then the corresponding term is (not) present in the model. The top two chromosomes are *parents*, $\gamma_{p_1} = 101010$ (blue) and $\gamma_{p_2} = 001011$ (green): they are mixed to spawn new models. We use a one–point cross over about the midpoint: the first half of γ_{p_1} is mixed with the second half of γ_{p_2} to produce two new offspring chromosomes, $\{\gamma_{c_1}, \gamma_{c_2}\}$. Mutation occurs probabilistically: each gene has a 25% chance of being mutated, e.g. a single gene (red) flipping from $0 \to 1$ to mutate γ_{c_2} to γ'_{c_2}. The next generation of the genetic algorithm will then include $\{\gamma_{c_1}, \gamma'_{c_2}\}$ (assuming γ_{c_1} does not mutate). To generate N_m models for each generation, $N_m/2$ parent couples are sampled from the previous generation and crossed over.

These concepts – shown in Fig. 2.1 – allow us to define

- *precision*: how precisely does $\hat{H}_i$ capture $\hat{H}_0$, i.e. if a term is included in $\mathcal{T}_i$ how likely it is to actually be in $\mathcal{T}_0$, Eqn 2.1a;
- *sensitivity*: how sensitive is $\hat{H}_i$ to $\hat{H}_0$, i.e. if a term is actually in $\mathcal{T}_0$, how likely $\mathcal{T}_i$ is to include it, Eqn. 2.1b.

$$\text{precision} = \frac{\text{TP}}{\text{TP} + \text{FP}} \tag{2.1a}$$

$$\text{sensitivity} = \frac{\text{TP}}{\text{TP} + \text{FN}} \tag{2.1b}$$

Informally, precision prioritises that predicted terms are correct, while sensitivity prioritises that true terms are identified. In practice, it is important to balance these considerations. F_β-score (Eq. (1.3)) is a measure which balances these, with weighting β in favour of sensitivity. In particular, F_1-score considers precision and sensitivity as equally important:

$$F_1 = \frac{2 \times (\text{precision}) \times (\text{sensitivity})}{(\text{precision} + \text{sensitivity})} = \frac{\text{TP}}{\text{TP} + \frac{1}{2}(\text{FP} + \text{FN})} =: f. \tag{2.2}$$

We give an example of these quantities in Fig. 2.1, where $\text{TP} = 3, \text{TN} = 4, \text{FP} = 1, \text{FN} = 2$, giving precision $= 3/4$ and sensitivity $= 3/5$, with a final $f = 0.67$, i.e. f is the average of the indicators of model quality we care about.

We adopt F_1-score as an indication of model quality because we are concerned both with precision and sensitivity of the models QMLA predicts as representations of Q. We can use F_1-score to measure the success of the algorithm, by recording f for all models in all generations, allowing us to see whether or not the approximation of the system is improving on average. Of course in realistic cases we can not assume knoweldge of $\mathcal{T}_o$ and therefore cannot compute F_1-score, but it is a useful tool in the development of the GES itself, or in cases where $\hat{H}_0$ is known, such as when the target system is simualated, e.g. in the case of device calibration. Our search for an effective OF can then be guided by seeking the method which most strongly improves the average F_1-score in test-cases. We will not use F_1-score within the algorithm[4], i.e. to inform any steps taken by QMLA, but simply to assess its performance independently.

2.1.2.1 *Distinguishing F_1-score through Bayes factors*

We have so far relied on Bayes factor (BF) as the means by which to distinguish models' ability to explain data from Q. We conjecture that models of higher F_1-score are usually statistically better at predicting dynamics of Q than those of lower F_1-score, and therefore BFs will favour models of higher F_1-score; Verifying this hypothesis will allow us to incorporate statistical tools

4 Except for meta-analysis in Section 2.1.3

Algorithm 2: ES subroutine: generate_models via genetic algorithm

Input: ν // information about models considered to date
Input: τ // truncation rate

Input: $g(\hat{H}_i)$ // objective function that can act on any model $\hat{H}_i$

Output: $\mathbb{H}$ // set of models

$N_m = |\nu|$ // number of models
for $\hat{H}_i \in \nu$ **do**
  $g_i \leftarrow g(\hat{H}_i)$ // model fitness via objective function
end

$r \leftarrow \text{rank}(\{g_i\})$ // rank models by their fitness
$\mathbb{H}_t \leftarrow \text{truncate}(r, N_m \times \tau)$ // truncate models by rank: only keep $N_m \times \tau$
$s \leftarrow \text{normalise}(\{g_i\})\ \forall \hat{H}_i \in \mathbb{H}_t$ // normalise remaining models' fitnesses
$\mathbb{H} = \{\}$ // new batch of chromosomes/models
while $|\mathbb{H}| < N_m$ **do**
  $p_1, p_2 = \text{roulette}(s)$ // use s to select two parents via roulette selection
  $c_1, c_2 = \text{crossover}(p_1, p_2)$ // produce offspring models
  $c_1, c_2 = \text{mutate}(c_1, c_2)$ // probabilistically mutate
  $\mathbb{H} \leftarrow \mathbb{H} \cup \{c_1, c_2\}$ // add new models to batch
end

return $\mathbb{H}$

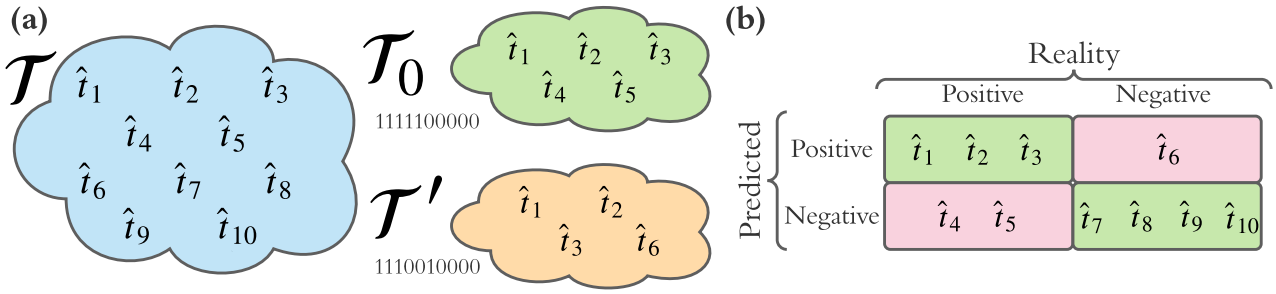

Figure 2.1: Concepts used for classification. **a**, the set of available terms $\mathcal{T}$ containing individual terms $\hat{t}_1$ to $\hat{t}_{10}$. The true model $\hat{H}_0$ is constructed from the set $\mathcal{T}_0$. Suppose a candidate $\hat{H}'$ has the set $\mathcal{T}'$. **b**, the confusion matrix for $\hat{H}'$. Correctly classified terms are true positives and true negatives (green), and incorrectly classified terms are false positives and true negatives (red).

into the design of OFs; we can perform straightforward tests training models of equally spaced F_1-score, and computing BF between all pairs.

In Fig. 2.2, we show the relationships between F_1-score and BF for various conditions. Firstly, under a standard training regime with full BF comparisons between all pairs, we see that in most cases, the model with higher F_1-score is favoured by BF. In Fig. 2.2b, we run a complete model training subroutine, but compute the BF based on fewer experiments and particles (retaining a fraction $N_p' = 0.2N_p$, $N_e' = 0.2N_e$ for comparisons). This verifies an earlier claim from **??**: although the strength of evidence is weaker given reduced BF resources, the direction of the evidence is usually the same, i.e. the insight is indicative of the true physics, so we can save considerable compute time by trusting these restricted BF calculations. On the other extreme, we see in Fig. 2.2**c**, where models are trained with – and BFs based upon – even greater resources than Fig. 2.2**a**, we see a similar effect: adding resources strengthens the evidence, but does not fundamentally change the outlook. Finally, in addition to reducing the resources used per BF calculation, we reduce the number of comparisons computed in Fig. 2.2**d**, as permitted when rating models according to the OF to be described in Section 2.2.7, or similar measures which can yield fitnesses from reduced data. Essentially we can see that the insight is largely the same from the most and least expensive training/comparison strategies, and by leveraging the available evidence (Fig. 2.2**d**), rather than brute-force computing as much evidence as possible (Fig. 2.2**a**), we can achieve similar results. Note that the time saving reported between full and partial connectivity between models scales with N_m: here, with $N_m = 10$, the former computes 45 BFs, while the latter computes 17; for $N_m = 60$, as used in full instances/runs presented in this chapter, these rise to 600 and 1770 respectively, so the benefit of the latter scheme is amplified.

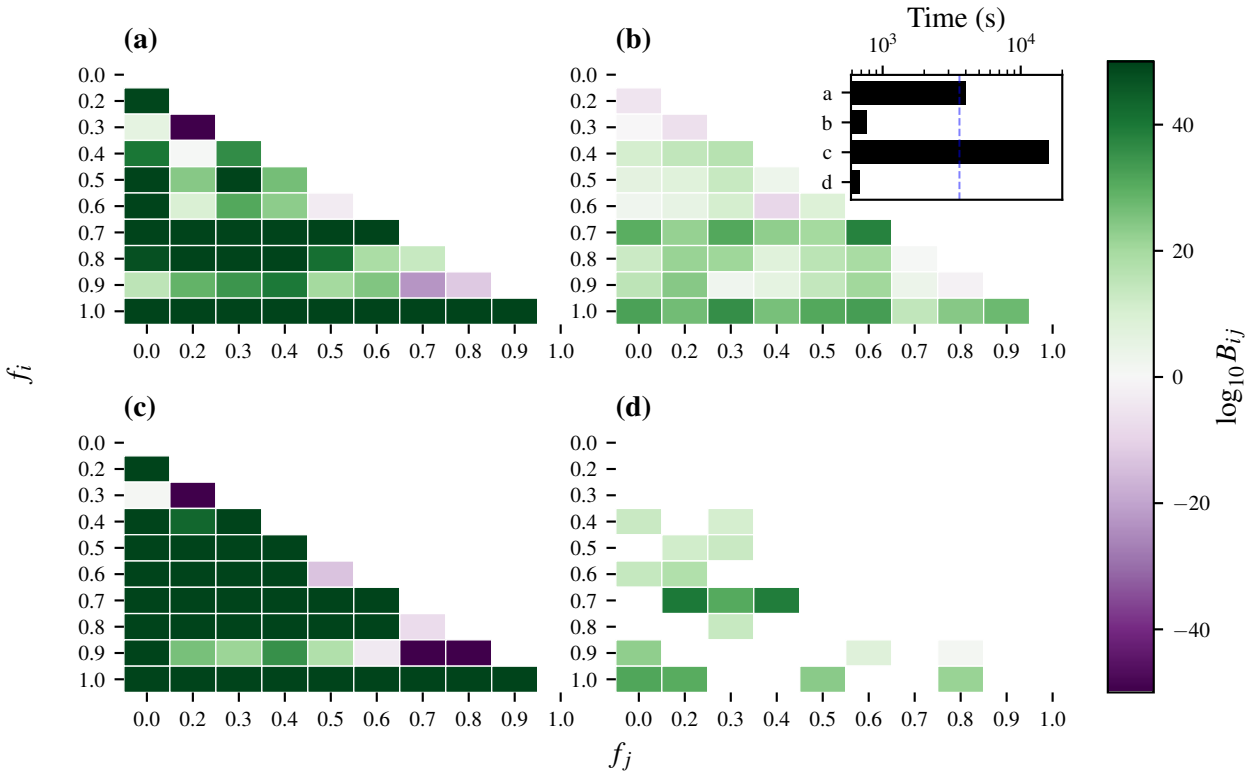

Figure 2.2: Pairwise Bayes factor, B_{ij}, by F_1-score of candidates $\hat{H}_i$ (f_i on the y-axis) and $\hat{H}_j$ (f_j on the x-axis). $\log_{10} B_{ij} > 0$ (< 0), green (purple), indicates statistical evidence that $\hat{H}_i$ ($\hat{H}_j$) is the better model with respect to the observed data. Visualisation is curtailed to $\log_{10} B_{ij} = \pm 50$. **a**, Models are trained with $N_e = 500, N_p = 2500$, and all available data is used in the calculation of BFs. **b**, $N_e = 500, N_p = 2500$ using only a fraction (0.2) of experiments/particles for BF calculations. **c**, $N_e = 1000, N_p = 5000$, using all available data in the calculation of BFs. **d**, $N_e = 500, N_p = 2500$, comparing only a subset of pairs of models through BFs, and using only a fraction (0.2) of experiments/particles for those calculations. This pairwise comparison strategy is used for the OF in Section 2.2.7. **Inset**, timings for each approach in seconds, with $t = 1$hr marked vertically in blue. Implementation details are listed in Table A.1

2.1.3 *Hyperparameter search*

Firstly we will validate our reasoning that F_1-score is a sensible figure of merit, by directly invoking it as the objective function. That is, we first implement a GA, using the mapping between models and chromosomes outlined above, where we fix the numbers of sites $d = 4$, and assume full connectivity between the sites, with $x-$, $y-$ and $z-$ couplings available, such that there are $N_t = 3 \times \binom{4}{2} = 18$ terms in $\mathcal{T}$, so that the total population is of size 2^{18} chromosomes. We can then sweep over the GA hyperparameters to find a suitable configuration: in Fig. 2.3 we show how the choice of parameters affect the success rate of preciesly identifying the target chromosome, which is chosen at random for each instance, and we run 20 instances of each configuration. The studied hyperparameters[5] are

i. number of generations;
ii. number of models per generation;
iii. mutation rate, r_m;
iv. number of generations for which a candidate must reign as the strongest observed, before the search terminates, the *cutoff*.

Naturally, we expect that running for more generations with more models per generation will result in a more effective search in the model space, having examined $N_g N_m$ models. We must also consider, however, that – in realistic cases of QMLA – the total computation time scales dramatically with these parameters, since training and comparing models are expensive subroutines. Our goal is therefore to identify the set of hyperparameters which best searches the model space while demanding the lowest N_g, N_m. We see that, unsurprisingly, the GA performs poorly when run with few resources, but broadly the performances are similiar provided it is run with sufficient resources. We can bound the parameters $r_m \geq 0.1, \text{cutoff} \geq 5, N_m \geq 16, N_g \geq 16$ to ensure a reasonable search through the model space, without having to consider a prohibitive number of models. We must bear in mind, however, that this parameter sweep refers only to the trivial case where the F_1-score is used as the OF, so we do not expect such high success rates in realistic cases.

2.2 OBJECTIVE FUNCTIONS

We have alluded to the central probelm in building a GA into QMLA: how to evaluate trained candidate models in the absence of a natural objective function (OF). In Sections 2.2.1 to 2.2.7 we will propose and analyse a number of potential OFs, some of which will underlie later studies in this thesis. We conclude this study by comparing the proposed OFs and selecting one for consideration in the remainder of this chapter; readers interested in the final application may prefer to skip to Section 2.2.8.

5 These and further hyperparameters can be swept using code within the QMLA codebase, in the directory scripts/-genetic_alg_param_sweep.

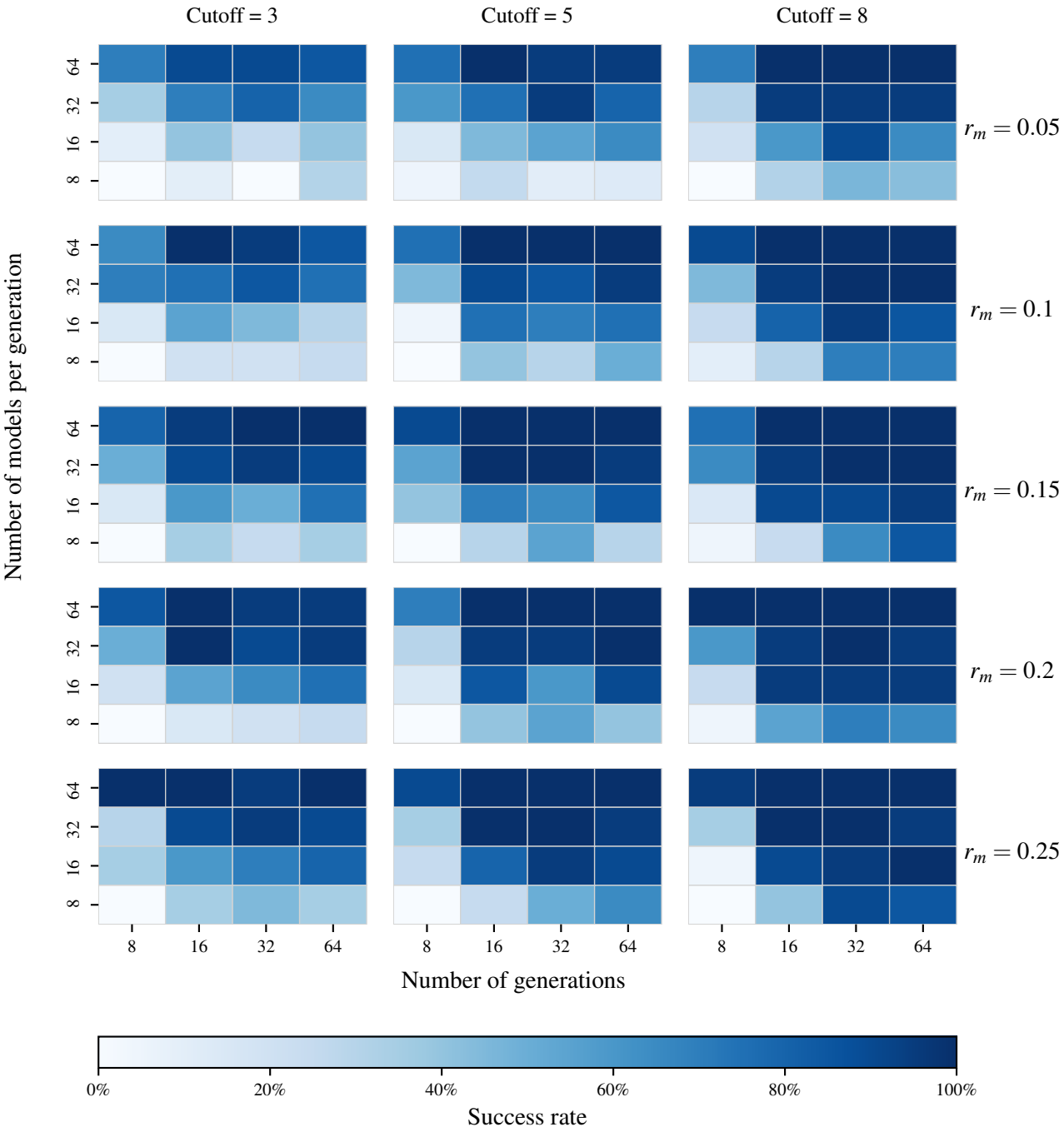

Figure 2.3: Genetic algorithm parameter sweep. Each subplot shows the success rates for varying numbers of generations, $N_G \in \{8, 16, 32, 64\}$, and numbers of models per generation, $N_m \in \{8, 16, 32, 64\}$. A subplot is generated for ranges of the mutation rate, r_m and the number of generations for which the elite model is unchanged after which the GA is cut off. Implementation details are listed in Table A.1

We will show how each OF computes a fitness, g_i, for candidate models, $\hat{H}_i$. For examples of each, we group together some demonstrative values in Table 2.2. For each $\hat{H}_i$, we may refer to

- $\mathcal{L}_i$, total log total likelihood (TLTL), introduced in **??**;
- k_i, the model's cardinality, i.e. number of terms in its parameterisation;
- $\mathcal{E}_i$, the bespoke set of experiments composed by the experiment design heuristic (**??**) solely for trainng $\hat{H}_i$;
- $n = |\mathcal{E}_i|$, the number of samples (datapoints) used in trainng $\hat{H}_i$.

In Table 2.2, we consider six randomly generated exemplary models – of varying quality with respect to the target, $\hat{H}_0$, listed in Eq. (2.3) – to demonstrate each OF's outcomes.

$$\begin{aligned}
\hat{H}_0 &= \hat{\sigma}^z_{(1,2)}\hat{\sigma}^z_{(1,3)}\hat{\sigma}^z_{(2,3)}\hat{\sigma}^z_{(2,5)}\hat{\sigma}^z_{(3,5)};\\
\hat{H}_a &= \hat{\sigma}^z_{(1,5)}\hat{\sigma}^z_{(3,4)}\hat{\sigma}^z_{(4,5)};\\
\hat{H}_b &= \hat{\sigma}^z_{(1,4)}\hat{\sigma}^z_{(1,5)}\hat{\sigma}^z_{(2,5)}\hat{\sigma}^z_{(3,4)};\\
\hat{H}_c &= \hat{\sigma}^z_{(1,2)}\hat{\sigma}^z_{(1,5)}\hat{\sigma}^z_{(2,4)}\hat{\sigma}^z_{(2,5)}\hat{\sigma}^z_{(4,5)};\\
\hat{H}_d &= \hat{\sigma}^z_{(1,3)}\hat{\sigma}^z_{(1,4)}\hat{\sigma}^z_{(1,5)}\hat{\sigma}^z_{(2,4)}\hat{\sigma}^z_{(2,5)}\hat{\sigma}^z_{(3,4)}\hat{\sigma}^z_{(3,5)};\\
\hat{H}_e &= \hat{\sigma}^z_{(1,2)}\hat{\sigma}^z_{(1,3)}\hat{\sigma}^z_{(1,5)}\hat{\sigma}^z_{(2,3)}\hat{\sigma}^z_{(2,5)}\hat{\sigma}^z_{(4,5)};\\
\hat{H}_f &= \hat{\sigma}^z_{(1,2)}\hat{\sigma}^z_{(1,3)}\hat{\sigma}^z_{(2,3)}\hat{\sigma}^z_{(2,4)}\hat{\sigma}^z_{(2,5)}\hat{\sigma}^z_{(3,4)}\hat{\sigma}^z_{(3,5)}.
\end{aligned} \tag{2.3}$$

2.2.1 *Inverse Log-likelihood*

$\mathcal{L}_i$, defined in **??**, can be thought of as a measure of the success of a given model at explaining data from any set of experiments, $\mathcal{E}$. This can be immediately interpreted as an OF, provided each candidate model computes a meaningful TLTL, requiring that they are all based on the same set of experiments, $\mathcal{E}_v$, which are designed explicitly for the purpose of model evaluation.

TLTL are negative and the strongest model has lowest $|\mathcal{L}_i|$ (or highest $\mathcal{L}_i$ overall), so the corresponding OF for candidate $\hat{H}_i$ is

$$g_i^L = \frac{-1}{\mathcal{L}_i}. \tag{2.4}$$

In our tests, Eqn. 2.4 is found to be too generous to poor models, assigning them non-negligible probability. Its primary flaw, however, is its reliance on $\mathcal{E}_v$: in order that the TLTL is significant, it must be based on meaningful experiments, the design of which can not be gauranteed in advance, or at least risks introducing strong bias towards some models.

Method		$\hat{H}_a$	$\hat{H}_b$	$\hat{H}_c$	$\hat{H}_d$	$\hat{H}_e$	$\hat{H}_f$
	F_1	0.0	0.2	0.4	0.5	0.7	0.8
	k	3	4	5	7	6	7
	$\overline{l_e}$	0.86 ± 0.29	0.84 ± 0.29	0.77 ± 0.27	0.78 ± 0.29	0.79 ± 0.26	0.79 ± 0.26
	$\mathcal{L}_i$	-143	-152	-131	-150	-125	-124
Inverse log-likelihood	g_i^L	0.00698	0.00659	0.00766	0.00669	0.00803	0.00804
	%	23	0	25	0	26	26
Akaike Info Criterion	AIC	293	311	271	313	261	263
	AICc	293	312	272	314	262	264
	w_i^A	1.81e-07	1.4e-11	0.00724	4.15e-12	1	0.334
	g_i^A	1.17e-05	1.03e-05	1.35e-05	1.01e-05	1.46e-05	1.43e-05
	%	22	0	25	0	27	26
Bayesian Info Criterion	BIC	301	322	284	331	277	281
	w_i^B	5.49e-66	1.26e-70	1.97e-62	1.11e-72	8.43e-61	8.95e-62
	g_i^B	1.11e-05	9.65e-06	1.24e-05	9.11e-06	1.31e-05	1.27e-05
	%	23	0	25	0	27	26
Bayes factor points	g_i^p	0	2	3	2	3	5
	%	0	13	20	13	20	33
Ranking	Ranking	6	4	3	5	2	1
	g_i^R	0	0.1	0.2	0	0.3	0.4
	%	0	10	20	0	30	40
Elo rating	Rating	909	944	1042	1007	1011	1084
	g_i^E	0	35	133	98	102	175
	%	0	0	26	19	20	34
Residuals	mean$\{\tilde{r_p^e}\}$	0.132	0.146	0.114	0.138	0.0858	0.0715
	g_i^r	0.753	0.729	0.785	0.743	0.836	0.862
	%	23	0	24	0	26	27

Table 2.2: Examples of how each objective function, g as described in Section 2.2.1 to Section 2.2.7, assign selection probability (denoted %) to the same set of candidate models, $\{\hat{H}_i\}$ listed in Eq. (2.3), when attempting to learn data from $\hat{H}_0$. Intermediate quantities, e.g. w_i^A, g_i^p are described in the section of the main text describing the corresponding OF. For each model we first summarise its F_1-score (Eq. (2.2)), number of terms k, median likelihood $\overline{l_e}$ (**??**), and total log total likelihood (TLTL) $\mathcal{L}_i$ (**??**), We use $n = 250$ samples, i.e. $\mathcal{L}_i$ is a sum of n likelihoods . The set of models is truncated so that only the strongest four are assigned selection probability.

2.2.2 *Akaike Information Criterion*

A common metric in the general field of model selection is Akaike information criterion (AIC) [32]. Incorporating TLTL, AIC objectively quantifies how well a given model accounts for data from the target system, and explicitly punishes models which use extraneous parameters by incurring a penalty on k_i. AIC is given by

$$AIC_i = 2k_i - 2\mathcal{L}_i. \tag{2.5}$$

In practice we use a slightly modified form of Eqn. 2.5 which corrects for the number of samples $n = |\mathcal{E}_i|$, called the Akaike information criterion corrected (AICC),

$$AICC_i = AIC_i + 2k_i \frac{k_i + 1}{n - k_i - 1}. \tag{2.6}$$

Model selection from a set of candidates occurs simply by selecting the model with lowest $AICC$. Following [**?**], by using Eqn. 2.6 as a measure of *relative likelihood* we retrieve selection probability via the *Akaike weights*,

$$w_i^A = \exp\left(\frac{AICC_{\min} - AICC_i}{2}\right), \tag{2.7}$$

where $AICC_{\min} = \min_i\{AICC_i\}$.

Akaike weights impose quite strong penalties on models which do not explain the data well, but also punish models with extra parameters, i.e. overfitting models, effectively searching for the strongest and simplest model simultaneously. The level of punishment for poorly performing models is likely too drastic: very few models will be in a range sufficiently close to $AICC_{\min}$ to receive a meaningful Akaike weight, suppressing diversity in the model population. Indeed, we can see from Table 2.2 that this results in most models being assigned negligible weight, which is not useful for parent selection. Instead we compute a straightforward quantity related to AIC,

$$g_i^A = \left(\frac{1}{AICc_i}\right)^2, \tag{2.8}$$

where we square the inverse AICC to amplify the difference in quality between models, such that stronger models are rewarded.

2.2.3 *Bayesian Information Criterion*

Related to the concept of AIC (Eqn. 2.5), is that of Bayesian information criterion (BIC),

$$BIC_i = k_i \, ln(n_i) - 2\mathcal{L}_i, \tag{2.9}$$

where k_i, n_i and $\mathcal{L}_i$ are as defined on Page 26. Analagously to Akaike weights, *Bayes weights* as proposed in §7.7 of [33], are given by

$$w_i^B = \exp\left(-\frac{BIC_i}{2}\right). \tag{2.10}$$

BIC is harsher than AIC in its punishment of models' cardinality k_i, demanding substantial statistical justification for the inclusion of more parameters. Again, this may be overly cumbersome for our use case: with such a relatively small number of parameters, the punishment is disproportionate. As with Akaike weights, rather than using Bayes weights directly, we opt for an OF related to them,

$$g_i^B = \left(\frac{1}{BIC_i}\right)^2. \tag{2.11}$$

2.2.4 *Bayes factor points*

A cornerstone of model selection within QMLA is the calculation of BFs (see **??**). We can compute the pairwise BF between two candidate models, B_{ij}, according to Eqn. **??**. B_{ij} can be based on some evaluation dataset, $\mathcal{E}_v$, but can also be calculated from $\mathcal{E}_i \cup \mathcal{E}_j$: this is a strong advantage since the resulting insight (Eqn. **??**) is based on experiments which were bespoke to both $\hat{H}_i, \hat{H}_j$. As such we can be confident that this insight accurately points us to the stronger of two candidate models.

We can utilise this facility by computing the BF between all pairs of models in a set of N_m candidates $\{\hat{H}_i\}$, i.e. compute $\binom{N_m}{2}$ BFs. Note that this is computationally expensive: in order to train $\hat{H}_i$ on $\mathcal{E}_j$ requires a further $|\mathcal{E}_j|$ experiments, each requiring N_P particles[6], where each particle corresponds to a unitary evolution and therefore the caluclation of a matrix exponential. The size of the model space is then quite a heavy disadvantage: examining N_g generations requires $N_g \times \binom{N_m}{2}$ BF calculations for complete assessment. In the case where all pairwise BF are performed, we can assign a point to $\hat{H}_i$ for every comparison in which it is deemed superior, according to **??**.

$$g_i^p = \sum_{j \in \mu} b_{ij}, \quad b_{ij} = \begin{cases} 1, & B_{ij} > 1 \\ 0, & \text{otherwise.} \end{cases} \tag{2.12}$$

This is a straightforward mechanism, but is overly blunt because it does not account for the strength of the evidence in favour of each model. For example, a dominant model will receive only a slightly higher selection probability than the second strongest, even if the difference between them was $B_{ij} = 10^{100}$. Further, the unfavourable scaling make this an expensive method.

6 Caveat the reduction in overhead outlined in **??**.

2.2.5 *Ranking*

Related to Section 2.2.4, we can rank models in a generation based on their number of BF points. BF points are assigned as in Eqn. 2.12, but instead of corresponding directly to fitness, we assign models a rank R, i.e. the model with highest g_i^p gets $R = 1$, and the model with n^{th} highest g_i^p gets $R = n$. Note here we truncate μ, meaning we remove the worse-performing models and retain only N'_m models, before calculating R, because computing R using all N_m models results in less distinct selection probabilities.

$$g_i^R = \frac{N'_m - R_i + 1}{\sum_{n=1}^{N'_m} n}, \tag{2.13}$$

where R_i is the ranking of $\hat{H}_i$ and N'_m is the number of models retained after truncation. Eq. (2.13) has a similary effect to Eq. (2.12) but awards higher selection probability to the strongest models. However, it too overlooks the nuanced perspective available through the total statistical evidence gathered by the series of BFs.

2.2.6 *Residuals*

Recall at each experiment, N_P particles are compared against a single experimental datum, d. By definition, d is the binary outcome of the measurement on Q under experimental conditions e. That is, d encodes the answer to the question: after time t under Hamiltonian evolution, did Q project onto the basis we have labelled $|d\rangle$ (usually the same as the input probe state $|\psi\rangle$)?

In practice we often have access to the complete likelihood, i.e. rather than a binary value, we have a number representing the probability that Q will project on to $d = 0$ for a given experiment e, $\Pr_Q(0|e)$. The likelihood – in this case equivalent to the expectation value – for Q is usually given by $\left|\langle\psi| e^{-i\hat{H}_0 t} |\psi\rangle\right|^2$. For consistency with QInfer [34] – on which QMLA's code base extends – we call the expectation value for the system $\Pr_Q(0)$; the same quantity can be computed for each particle, called $\Pr_p(0)$. Likewise, we can simulate this quantity for each particle, $\Pr_p(0|e)$. This allows us to calculate the *residual* between the system and individual particles' likelihoods, r_p^e; we can hence compute the mean residual across all particles in a single experiment r^e:

$$\begin{aligned} r_p^e &= \left| Pr_Q(0|e) - Pr_p(0|e) \right| \\ r^e &= \underset{p}{\text{mean}}\{r_p^e\} \end{aligned} \tag{2.14}$$

Residuals capture how closely the particle distribution reproduced the dynamics from Q: $r_p^e = 0$ indicates perfect prediction, while $r_p^e = 1$ is completely incorrect. We can therefore maximise the quantity $1 - r$ to find the best model, using the OF

$$g_i^r = |1 - \underset{e \in \mathcal{E}}{\text{mean}}\{r^e\}|^2. \tag{2.15}$$

This OF can be thought of in frequentist terms as similar to the residual sum of squares, although instead of summing the residual squares, we take the average to ensure $0 \leq r \leq 1$. g_i^r encapsulates how well the candidate model reproduces a paticular set of dynamics from the target system, as a proxy for how well that candidate describes the system. This is not always a safe figure of merit: in most cases, we do not expect parameter learning to perfectly optimise $\vec{\alpha}_i$. Reproduced dynamics alone can not capture the prospect that $\hat{H}_i = \hat{H}_0$, but rather inform statistical measures such as BF that allow us to make qualified statements about the system.

This OF provides a useful test for QMLA's GA: by simulating the case where parameters *are* learned perfectly, such that we know that g_i^r truly represents the ability of $\hat{H}_i$ to simulate $\hat{H}_0$, then this OF gaurantees to promote the strongest models, especially given that $\hat{H}_i = \hat{H}_0 \implies r_p^e = 0 \; \forall \; \{e, p\}$. In realistic cases, however, the non-zero residuals – even for strong $\hat{H}_i$ – may arise from imperfectly learned parameters, rendering the usefulness of this OF uncertain. Finally, it does not account for the cardinality, k_i, of the candidate models, which all ML protocols aim to avoid in general; this could result in favouring severely overfitting models in order to gain marginal improvement in residuals.

2.2.7 *Bayes factor enhanced Elo-ratings*

A popular tool for rating individual competitors in sports and games is the *Elo rating* scheme, e.g. used to rate chess players and soccer teams [35, 36], also finding application in the study of animal hierarchies [37]. Elo ratings allow for evaluating the relative quality of individuals based on incomplete pairwise competitions, e.g. despite two football teams having never played against each other before, it is possible to quantify the difference in quality between those teams, and therefore to predict a result in advance [38]. There is a direct a parallel between these types of competitions and QMLA: we similarly have a pool of individual competitors (models), which we can place in direct competition, and quantify the comparitive outcome through BF, in order to determine the strongest.

Elo ratings are transitive: given some interconnectivity in a generation, we need not compare *every* pair of models in order to make meaningful claims about which are strongest; it is sufficient to perform a subset of comparisons, ensuring each individual undergoes robust competition. We can take advantage of this transitivity to reduce the combinatorial overhead usually associated with computing bespoke BFs between all models (i.e. using their own training data $\mathcal{E}_i$ instead of a generic $\mathcal{E}_v$). In practice, we map N_m models within a generation to vertices on a regular graph of degree $nicefrac N_m 3$, i.e. each model is connected to $N_m/3$ other models within μ. Models

which share an edge then undergo BF comparison. For example, with $N_m = 60$ this leads to 600 BF calculations, compared with 1770 calculations in the fully connected graph. While every pair of models $(\hat{H}_i, \hat{H}_m)$ are not directly connected, there is always a chain of length $l \leq l_{max}$ edges between them. For $N_m = 60$, we find $l_{max} = 2$, e.g. for $\hat{H}_i, \hat{H}_k$ disconnected, there are comparisons $(\hat{H}_i, \hat{H}_j), (\hat{H}_j \hat{H}_k)$.

The Elo rating scheme is a nonlinear points transfer system, as follows: upon creation, $\hat{H}_i$ is assigned a rating R_i; every comparison with a competitor $\hat{H}_j$ results in B_{ij}; R_i is updated according to the known strength of its competitor, R_j, as well as the result B_{ij}. The Elo update ensures that winning models are rewarded for defeating another model, but that the extent of that reward reflects the quality of its opponent. As such, this is a fairer mechanism than BF points, which award a point for every victory irrespective of the opposition: if $\hat{H}_j$ is already known to be a strong or poor model, then ΔR_i proportionally changes the credence we assign to $\hat{H}_i$. It achieves this by first computing the *expected* result of a given comparison with respect to each model, based on the current ratings,

$$E_i = \frac{1}{1 + 10^{\frac{R_j - R_i}{400}}}; \tag{2.16a}$$

$$E_i + E_j = 1, \tag{2.16b}$$

Then, we find the binary *score* from the perspective of each model,

$$\begin{cases} B_{ij} > 1 & \Rightarrow \; S_i = 1; \; S_j = 0 \\ B_{ij} < 1 & \Rightarrow \; S_i = 0; \; S_j = 1 \end{cases} \tag{2.17}$$

which is used to determine the change to each model's rating,

$$\Delta R_i = \eta \times (S_i - E_i) \,. \tag{2.18}$$

An important detail is the choice of η, i.e. the *weight* of the change to the models' ratings. In standard Elo schemes this is a fixed constant, but here – taking inspiration from football ratings where η is the number of goals by which one team won – we weight the change by the strength of our belief in the outcome: $\eta \propto |B_{ij}|$. That is, similarly to the interpretation of Eqn. **??**, we use the evidence in favour of the winning model to transfer points from the loser to the winner, albeit we temper the effect by instead using $\eta = \log_{10}(B_{ij})$, since BF can give very large numbers. In total, then, following the comparison between models $\hat{H}_i, \hat{H}_j$, we can perform the Elo rating update

$$R_i' = R_i + \log_{10}(B_{ij}) \left(S_i - \frac{1}{1 + 10^{\frac{R_j - R_i}{400}}} \right). \tag{2.19}$$

This procedure is easiest to understand by following the example in Table 2.3.

7 Note to achieve $B_{ij} = 10^{100} = e^{\mathcal{L}_i - \mathcal{L}_j} \implies \mathcal{L}_i - \mathcal{L}_j = ln(10^{100}) \approx 7$.

Model		R_i	E_i	S_i	B_{ij}	$\log_{10}(B_{ij})$	ΔR_i	R'_i
$\hat{H}_a > \hat{H}_b$	$\hat{H}_a$	1000	0.76	1	1e+100	100	0.24	1024.0
	$\hat{H}_b$	800	0.24	0	1e-100	100	-0.24	776.0
$\hat{H}_b > \hat{H}_a$	$\hat{H}_a$	1000	0.76	0	1e-100	100	-0.76	924.0
	$\hat{H}_b$	800	0.24	1	1e+100	100	0.76	876.0

Table 2.3: Example of Elo rating updates. We have two models, where $\hat{H}_a$ is initially believed to be a stronger candidate than $\hat{H}_b$, i.e. has a higher starting Elo rating, R_i. We demonstrate the effect when there is strong evidence[7] in favour of either model through BF comparison, $B_{ij} \sim 10^{100}$. In the first case, $\hat{H}_a$ defeats $\hat{H}_b$, as firmly expected according to their initial ratings, so the corresponding reward (cost) for $\hat{H}_a$ ($\hat{H}_b$) is relatively small. In the second case, contrary to prediction $\hat{H}_b$ outperforms $\hat{H}_a$, so $\hat{H}_b$ receives a large share of Elo points from $\hat{H}_a$.

Finally, it remains to select the starting rating R_i^0 to assign models upon creation. Although this choice is arbitrary, it can have a strong effect on the progression of the algorithm. Here we impose details specific to the QMLA GA: at each generation we admit the top two models automatically for consideration in the next generation, such that strongest models can stay alive in the population and ultimately win. These are called *elite* models, $\hat{H}_e^1, \hat{H}_e^2$. This poses the strong possibility for a form of generational wealth: if elite models have already existed for several generations, their Elo ratings will be higher than all alternatives by defintion. Instead, we would prefer that newly spawned models can overtake the Elo rating of elite models. To resolve this, at each generation, all models – including $\hat{H}_e^1, \hat{H}_e^2$ – are assigned the same initial rating, $R_i^0 = 1000$.

In order to derive a meaningful selection probability for each candidate, we must first ground the raw Elo rating at each generation μ: we subtract the lowest rating among the entertained models, R_{min}^{μ}. This serves to ensure the range of remaining R_i represent only by the difference between models as assessed within μ: a very strong model might have much higher R_i than its contemporaries, but that difference was earned exclusively by comparison within μ, so it is deserving of its higher fitness and therefore greater selection probability. We perform this step before truncation[8], so that the models remaining post-truncation all have non-zero fitness. Finally, then, we name this OF the *Bayes factor enhanced Elo ratings (BFEER)*: the fitness of each model $\hat{H}_i^{\mu} \in \mu$ is attained directly from its rating R_i after undergoing Elo updates based on BFs in the current generation, minus the minimum rating of any model in the same generation R_{min}^{μ},

$$g_i^E = R_i^{\mu} - R_{\text{min}}^{\mu}. \tag{2.20}$$

8 We truncate the N_m models on μ by the truncation rate τ, i.e. only τN_m models are considered as potential parents in the GA. In this chapter we use $\tau = 1/3$.

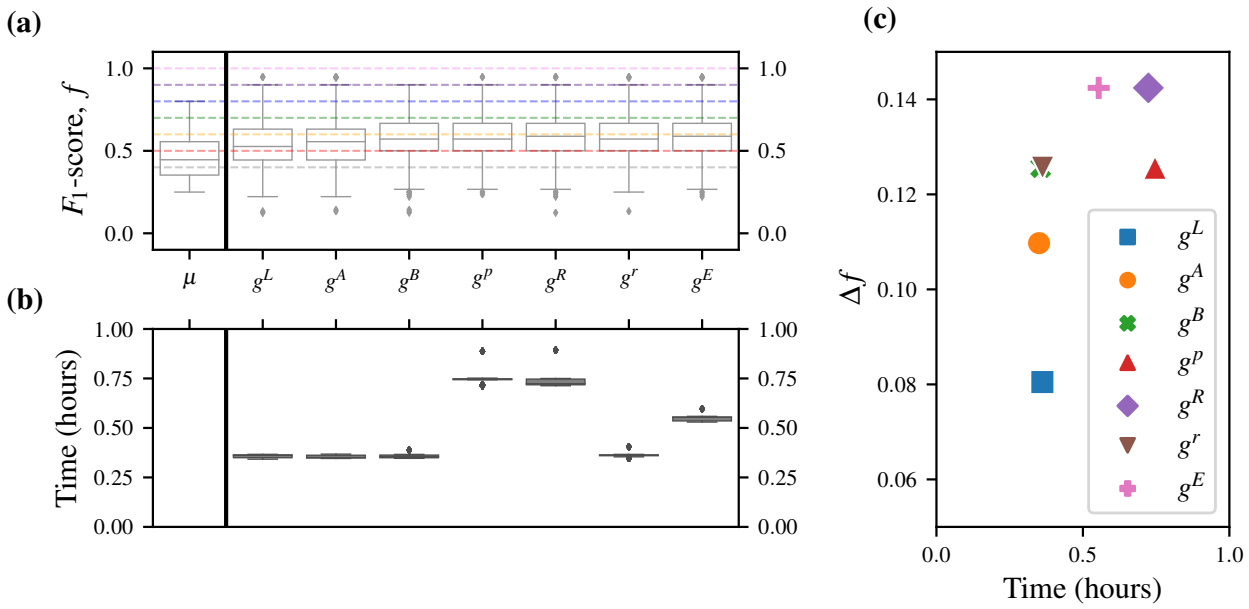

Figure 2.4: Comparison between proposed objective functions (OFs). Each OF trains the same initial generation of $N_m = 28$ models with resources $N_E = 500, N_P = 2000$, and then design a new set of N_m models through a roulette strategy, such that the only difference between OF's output is how they assign selection probability. We run each OF 25 times for the same target system, a 4–qubit Heisenberg–XYZ model. **(a)** shows the box–plot of spawned models' F_1-score, f, where the median and inter–quartile ranges are indicated by the boxes, as well as those of the initial generation μ centered on $f_\mu = 0.45$. We mark $f = \{0.4, 0.5, ..., 1.0\}$ for ease of interpretation. **(b)** shows box–plots of the time taken to compute the single generation in each case. In **(c)** we report the difference between the median f among the newly proposed models from f_μ, Δf, plotted against the time to achieve the result.

The advantage of this OF is that it gives a meaningful value on the absolute quality of every model, allowing us to determine the strongest, and importantly to find the relative strength between models. Further, it exploits bespoke BFs, i.e. based on the considered models' individually designed $\mathcal{E}_i$, removing the impetus to design $\mathcal{E}_v$ which can evaluate models definitively. One disadvantage is that it does not explicitly punish models based on their cardinality, however this feature is partially embedded by adopting BF for the comparisons, which are known to protect against overfitting [39].

2.2.8 *Objective function selection*

Having proposed a series of possible objective functions, we are now in a position to analyse their appropriateness in the context of QMLA. Recall from Section 2.1.2 that we use F_1-scoreas

the figure of merit against which individual models are measured; we can compare OFs on the basis of the F_1-scoreof models they spawn.

First we can remark on the examples listed in Table 2.2. The OFs which rely on the TLTL, i.e. g^L, g^A, g^B, g^r, are effectively tricked by the log-likelihood, which appears reasonably convincing for poor models, e.g. $\hat{H}_a, \hat{H}_c$. This underlines the risk in buidling $\mathcal{E}_v$, which can be biased towards weak models, for example resulting in high selection probability for $\hat{H}_a$ which has $f = 0$, while $\hat{H}_d$, with $f = 0.4$ is discarded. On the other hand, OFs grounded by the BF (g^p, g^R, g^E) invariably promote models of higher F_1-score, justifying the role of statistical evidence used for those calculations. Overall, however, the insights from this complete example are insufficient to make general claims about the performance of each OF, so here we examine their outputs systematically.

Returning to the task of determining our favoured OF, we choose some random target $\hat{H}_0$, and run a single generation of the GES with each OF, allowing us to assess their performance based on the quality of models the GA produces under their respective guidance. We train the same batch of $N_m = 28$ random models in each case, and allow each OF to compute the selection probabilities for those models, and therefore direct the design of the hypothetical next generation of models. We plot the distribution of F_1-score that each OF produces in Fig. 2.4, also accounting for the time taken in each case, i.e. we report the time to train and evaluate the single generation on a 16–core node.

Overall, then, we can see that a strong balance of outcome with resource considerations are achieved by the BFEER strategy, Section 2.2.7, so we will use it for the case study presented in this chapter. We strongly emphasise, however, that the performance of each objective function can vary under alternative conditions, and therefore similar analysis may be warranted for future applications. For instance, if $t_{\max}$ is known to be small, in smaller model spaces, using g^r results in higher success rates. We retain BFEER, however, for generality and novelty, but it is important to recognise that the results listed do not reflect an upper limit of QMLA's performance, but rather reflect the constraints of the system under study; each Q will bring its own unique considerations which can result in significantly stronger or weaker performance under each OF. In particular, we will later use the residual OF, Section 2.2.6, to study a larger model space under assumptions of perfect parameter learning, **??**.

2.3 APPLICATION

Having introduced all the necessary concepts of GAs, mapped them to the QMLA framework and chosen a suitable OF, we can finally use the GES for model search. In summary of this chapter so far, we use the following settings.

- Models are mapped to a unique bit string (chromosome), where each bit represents whether a given model term (gene) is present; chromosomes are of length N_t genes.
- A maximum of N_g generations are run, each with N_m unique models.

- Candidate models are trained using QHL, specifically by using interactive quantum likelihood estimation (IQLE)[9] for parameter estimation.
- Models' fitness are determined by their BFEER, after having been trained by QHL and compared against some set of competing candidate models.
- For generating models on $\mu + 1$, the models on μ are first truncated with truncation rate τ; the remaining τN_m models are assigned selection probability based on their fitness.
- Pairs of models are selected to become parents sequentially using roulette selection. Highly favoured models can parent many offspring models.
- Selected parent models are crossed over via a one-point cross-over, at crossover location $\kappa \in \left(\frac{N_t}{4}, \frac{3N_t}{4}\right)$, and probabilistically mutated with rate $r_m = 0.25$.
- The top two elite models from μ are included on the subsequent generation $\mu + 1$.
- If, after 5 generations, the highest-fitness (elite) model is unchanged, i.e. $\hat{H}_e^{\mu} = \hat{H}_e^{\mu+5}$, we terminate the search and declare that model as the champion, $\hat{H}' = \hat{H}_e^{\mu}$.
- Otherwise, after N_g generations, the highest-fitness model on the final generation is declared the global champion model, $\hat{H}' = \hat{H}_C^{N_g}$.

We will use a four-qubit model space under the Heisenberg formalism, **??**, such that any pair of sites $\langle k, l \rangle$ can be coupled by any of the terms $\{\hat{\sigma}^x_{\langle k,l\rangle}, \hat{\sigma}^y_{\langle k,l\rangle}, \hat{\sigma}^z_{\langle k,l\rangle}\}$, so in total there are $N_t = |\mathcal{T}| = 3 \times \binom{4}{2} = 18$ terms, giving a model space of $2^{18} \approx 250,000$ viable models/chromosomes. For practical reasons[10], we set $N_m = 60$ and $N_g = 16$, although in most cases the elitism clause is triggered so the search terminates long before N_g is reached. The true parameters $\vec{\alpha}_0$ are assigned randomly in the range $(0.25, 0.75)$; within QHL the prior is set as a multivariate normal distribution 0.5 ± 0.125. We choose $\hat{H}_0$ at random to contain half the available terms[11],

$$\hat{H}_0 = \hat{\sigma}^{yz}_{(1,2)}\hat{\sigma}^{z}_{(1,3)}\hat{\sigma}^{y}_{(1,4)}\hat{\sigma}^{xy}_{(2,3)}\hat{\sigma}^{x}_{(2,4)}\hat{\sigma}^{xz}_{(3,4)}. \tag{2.21}$$

2.3.1 *Analysis*

We will analyse the GES from four perspectives: a single model, a single generation, a single QMLA instance, and the overall performance across many instances, i.e. a run.

Recall that BFEER are mediated through random graphs: given N_m models on μ, a given model $\hat{H}_i$ undergoes some $N_i^{BF} < N_m$ BF comparisons. In Fig. 2.5 we show the BF results and

9 IQLE assumes complete access to the target system, see **??**. This restricts the present analysis to simulateable, rather than physical, use cases, e.g. device calibration.

10 This is to ensure, with 15 available worker nodes, and accounting for some slowly-learning models, that all N_m models in a generation are trained within $4t_{\text{qhl}}$, where t_{qhl} is the time to train a single model.

11 Note we use a compact model representation, e.g. $\hat{H}_i = \hat{\sigma}^{yz}_{(1,2)}\hat{\sigma}^{z}_{(1,3)} = \hat{\sigma}^{y}_{(1,2)} + \hat{\sigma}^{z}_{(1,2)} + \hat{\sigma}^{z}_{(1,3)}$.

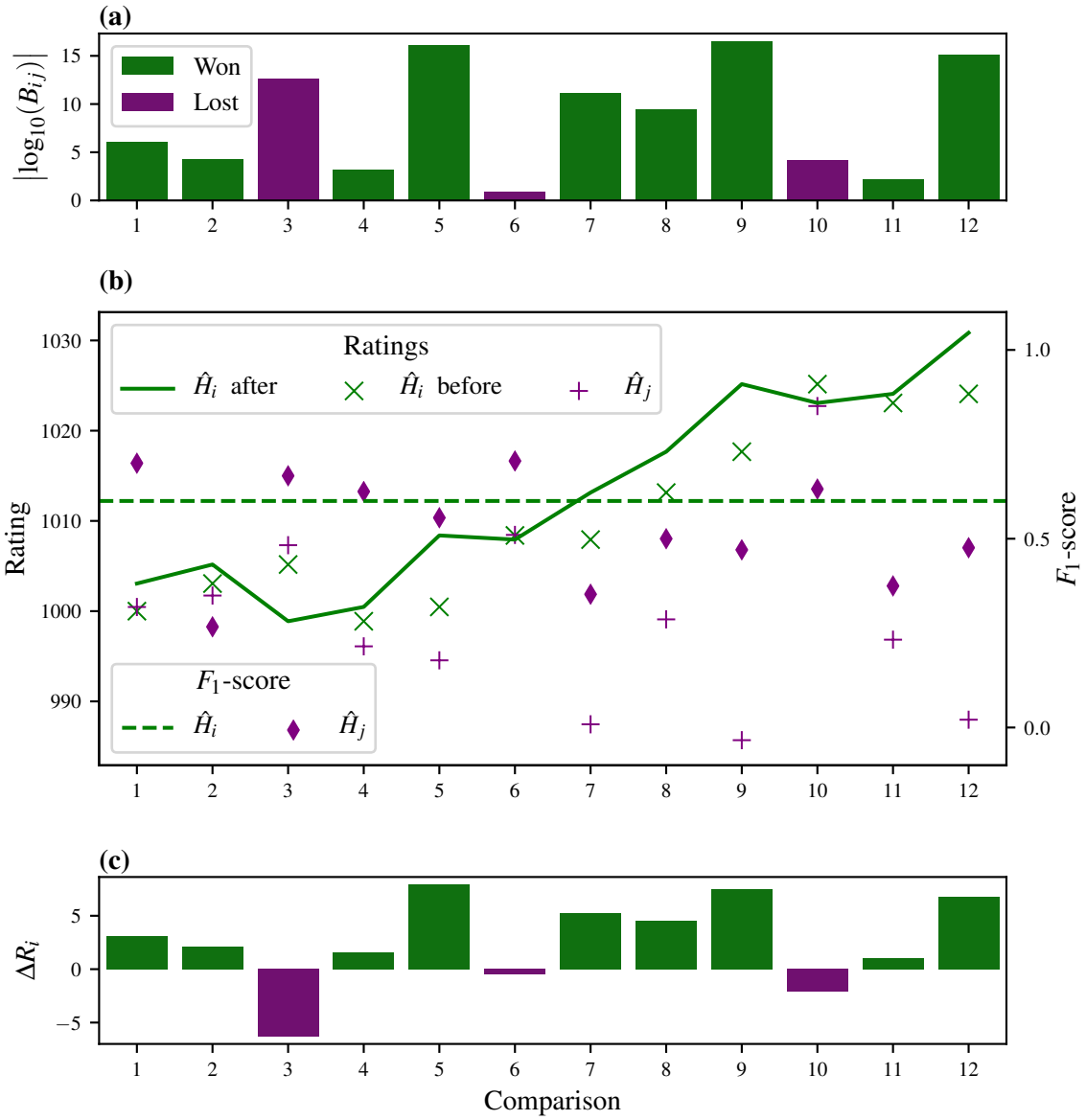

Figure 2.5: Progression of Bayes factor enhanced Elo ratings for a single candidate, $\hat{H}_i$, within a single generation. **a**, The BFs between $\hat{H}_i$ and some opponents, $\{\hat{H}_j\}$, from the perspective where $\hat{H}_i$ *wins* given $B_{ij} > 1 \Rightarrow \log_{10} B_{ij} > 0$, and *loses* otherwise. **b**, $\hat{H}_i$'s rating is shown (solid green line) changing according to the BFs comparisons with 12 other models from the same generation. Before each comparison, $\hat{H}_i$'s rating is shown (green cross) as well as the rating of its opponent, $\hat{H}_j$ (purple plus). The F_1-scores are also shown for $\hat{H}_i$ (dashed green line) and $\hat{H}_j$ (purple diamond). **c**, The corresponding change in $\hat{H}_i$'s rating, ΔR_i. Implementation details are listed in Table A.1

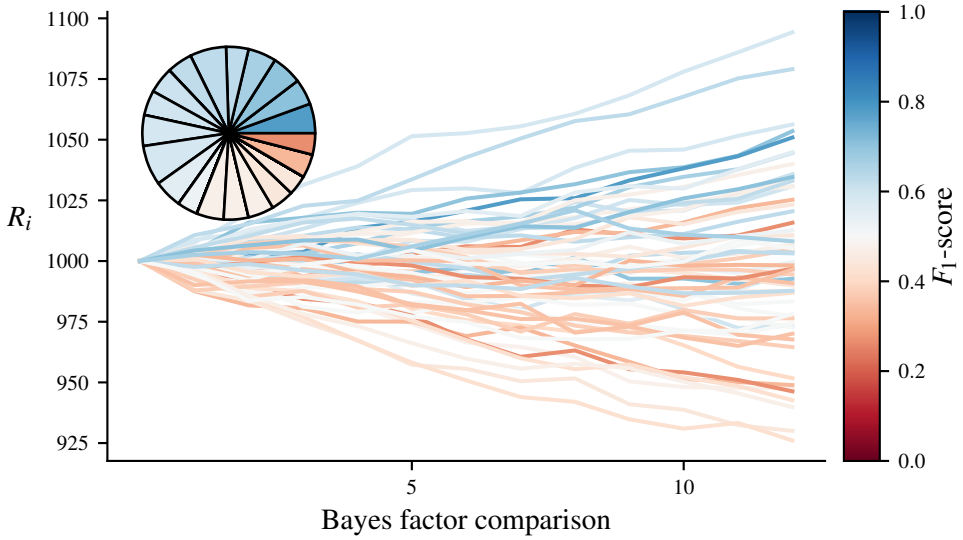

Figure 2.6: Ratings of all $N_m = 60$ models in a single genetic algorithm generation. Each line represents a unique model and is coloured by the F_1-score of that model. **Inset**, the selection probabilities resulting from the final ratings of this generation. Only $tau = 1/3$ of models are assigned selection probability, while the remaining poorer-performing models are discarded. Implementation details are listed in Table A.1

effects on the rating of a random model, $\hat{H}_i$, where $N_m = 60$ and $N_i^{BF} = 12$, i.e. $\hat{H}_i$ is directly compared against $\sim 20\%$ of contemporary models on μ. We see that $\hat{H}_i$'s rating is effected by whether it wins a given comparison, but also by the strength of evidence provided by the comparison (the BF), and the quality of its opposition $\hat{H}_j$, i.e. the initial rating of $\hat{H}_j$. For example, the sixth comparison finds $\hat{H}_j$ as the superior model, but the evidence is relatively weak and $\hat{H}_i, \hat{H}_j$ began with similar ratings, so R_i is not effected drastically.

We extend the single model analysis of Fig. 2.5 to all N_m models in the first generation in Fig. 2.6. The general trend is that models of higher F_1-score have their ratings increased, at the expense of models of lower F_1-score. After assessing models thus, the set of models is truncated with rate $\tau = 1/3$ to retain only the strongest 20 candidates, which are assigned selection probability, i.e. their chance of being chosen to become a parent during roulette selection, as in Section 1.3.3. N_m models are required to populate the next generation: the two models with highest R_i – the *elite* models – are automatically granted a position; the remaining positions are filled through the crossover procedure outlined above.

Similarly we can consider the quality and ratings of models across generations. In Fig. 2.7**(a)** we see the ratings for models over an entire QMLA instance: the trend suggested by Fig. 2.6 continues, where models of higher F_1-score tend to achieve higher BFEER. The gene pool as a whole tends towards a homogeneous set of high-quality models, all with $f \geq 0.85$, Fig. 2.7**(b)**.

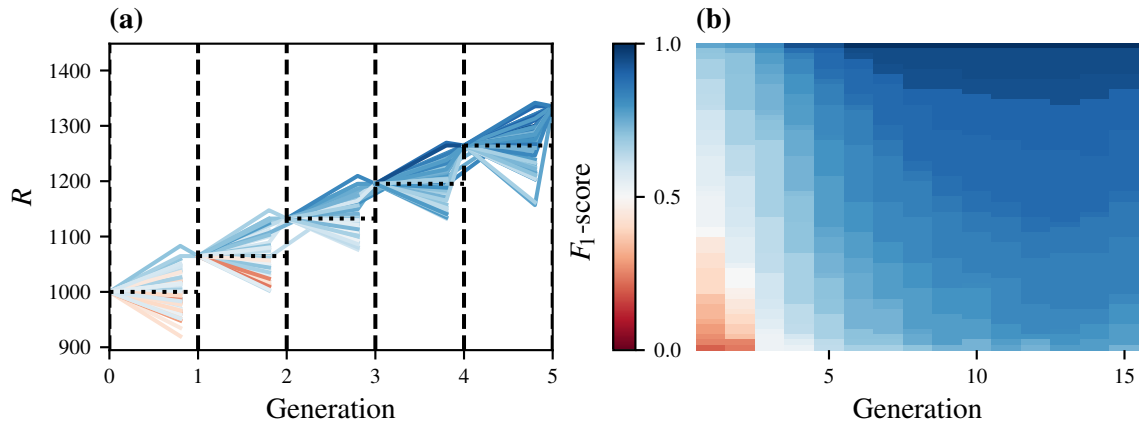

Figure 2.7: A single instance of the QMLA ga. **a**, Ratings of all models for the first five generations. Each line in each generation represents a model by its F_1-score. Horizontal dotted lines show the starting rating at that generation. **b**, Gene pool progression for $N_m = 60, N_g = 15$. Each tile at each generation represents a model by its F_1-score. Implementation details are listed in Table A.1

Consequently, even in cases where the precise model, $\hat{H}_0$, is not identified, the champion model is highly informative, in that it captures many of the same interactions, therefore most-likely providing meaningul insight on the system's physics.

Finally, to understand the performance of the QMLA algorithm overall, we run 100 independent instances in a run, Fig. 2.8. We see that, while the overall model space can be characterised by the distribution of models' F_1-score, where we sample where $\bar{f} = 0.5 \pm 0.14$, that QMLA quickly moves to the subspace of high-quality models, i.e. the models explored have median $f = 0.76 \pm 0.15$. This exploration is based on 430 ± 45 chromosomes per instance, i.e. QMLA trains only 0.16% of the 2^{18} potential models. Ultimately QMLA nominates champion models, $\{\hat{H}'\}$ with $f \geq 0.88$ in all instances, and precisely identifies $\hat{H}' = \hat{H}_0$ in 72% of instances. Considering the big picture, where the remit of QMLA is to identify the interactions the target system is subject to, we show how often each term/gene is included in $\hat{H}'$ in Fig. 2.8**d**. Crucially, we see that terms which really are within the true Hamiltonian, $\hat{t} \in \mathcal{T}_0$, are found significantly more frequently than those without, $\hat{t} \notin \mathcal{T}_0$. This level of analysis can be used to post-validate the outcome of QMLA, i.e. rather than relying on $\hat{H}'$ from a single instance, trusting the terms' individual frequencies as evidence that they are of importance when describing the system of interest.

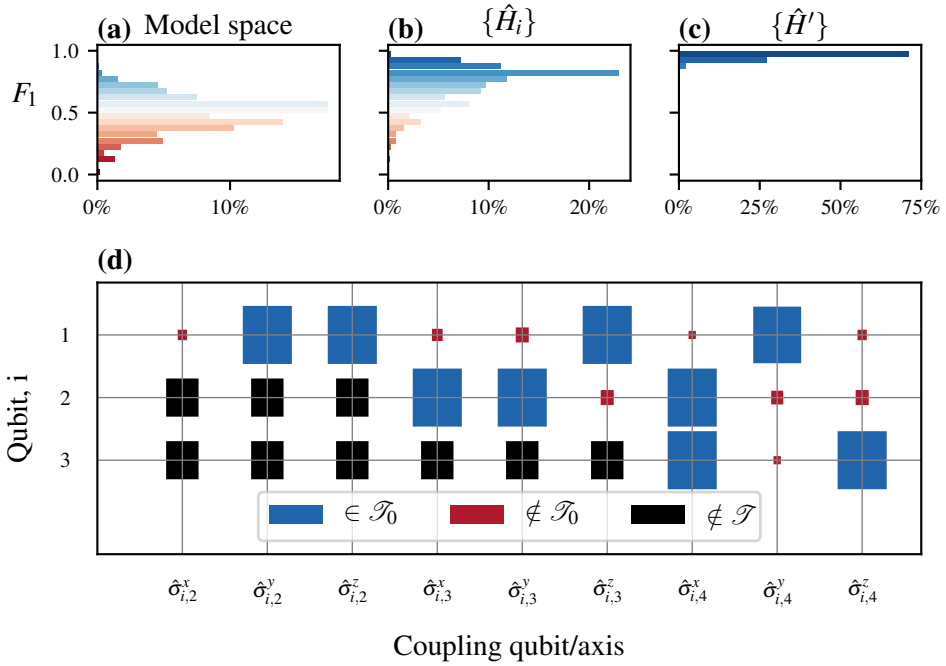

Figure 2.8: A run of the QMLA genetic algorithm (GA), consisting of 100 independent instances. **(a)**, The model space contains $2^{18} \approx 250,000$ candidate models; normally distributed around $f = 0.5 \pm 0.14$. **(b)**, The models explored during the model search of all instances combined, $\{\hat{H}_i\}$, show that QMLA tends towards stronger models overall, with $f = 0.76 \pm 0.15$ from $\sim$ 43,000 chromosomes across the instances, i.e. each instance trains $\sim$ 430 distinct models. **(c)**, Champion models from each instance, showing QMLA finds strong models in general, and in particular finds the true model $\hat{H}_0$ (with $f = 1$) in 72% of cases, and $f \geq 0.88$ in all instances. **(d)**, Hinton diagram showing the rate at which each term is found in the winning model. The size of the blocks show the frequency with which they are found, while the colour indicates whether that term was in the true model (blue) or not (red). Terms are couplings between two qubits, e.g $\hat{\sigma}^x_{(1,3)}$ couples the first and third qubits along the x-axis. We test four qubits with full connectivity, resulting in 18 unique terms (terms with black rectangles are not considered by the GA). Implementation details are listed in Table A.1

2.3.2 *Device characterisation*

This adaptive GES may prove a useful application of QMLA in the domain of device calibration, in particular to characterise some untrusted quantum simulator. That is, by using the simulator to implement some target $\hat{H}_0$, QMLA can identify which operator is *actually* implemented. For instance, implementation of a four–qubit model relies on high-fidelity two-qubit gates between arbitrary qubit pairs, and QMLA can effectively reconstruct which operations were and were not faithfully computed.

APPENDIX

A

FIGURE REPRODUCTION

Most of the figures presented in the main text are generated directly by the QMLA framework. Here we list the implementation details of each figure so they may be reproduced by ensuring the configuration in Table A.1 are set in the launch script. The default behaviour of QMLA is to generate a results folder uniquely identified by the date and time the run was launched, e.g. results can be found at the *results directory* qmla/Launch/Jan_01/12_34. Given the large number of plots available, ranging from high-level run perspective down to the training of individual models, we introduce a plot_level $\in \{1, ..., 6\}$ for each run of QMLA: higher plot_level informs QMLA to generate more plots.

Within the results directory, the outcome of the run's instances are stored, with analysis plots broadly grouped as

- evaluation: plots of probes and times used as the evaluation dataset.
- instances: outcomes of an individual QMLA instance, grouped by the instance ID. Includes results of training of individual models (in model_training), as well as sub-directories for anlaysis at the branch level (in branches) and comparisons.
- combined_datasets: pandas dataframes containing most of the data used during analysis of the run. Note that data on the individual model/instance level may be discarded so some minor analyses can not be performed offline.
- exploration_strategy_plots plots specifically required by the ES at the run level.
- champion_models: analysis of the models deemed champions by at least one instance in the run, e.g. average parameter estimation for a model which wins multiple instances.
- performance: evaluation of the QMLA run, e.g. the win rate of each model and the number of times each term is found in champion models.
- meta analysis of the algorithm' implementation, e.g. timing of jobs on each process in a cluster; generally users need not be concerned with these.

In order to produce the results presented in this thesis, the configurations listed in Table A.1 were input to the launch script. The launch scripts in the QMLA codebase consist of many configuration settings for running QMLA; only the lines in snippet in Listing A.1 need to be set according to altered to retrieve the corresponding figures. Note that the runtime of QMLA grows quite quickly with N_e, N_p (except for the AnalyticalLikelihood ES), especially for the entire QMLA algorithm; running QHL is feasible on a personal computer in < 30 minutes for $N_e = 1000; N_p = 3000$.

```
#!/bin/bash
```

```
###############
# QMLA run configuration
###############
num_instances=1
run_qhl=1 # perform QHL on known (true) model
run_qhl_mulit_model=0 # perform QHL for defined list of models.
exp=200 # number of experiments
prt=1000 # number of particles

###############
# QMLA settings
###############
plot_level=6
debug_mode=0

###############
# Choose an exploration strategy
###############

exploration_strategy='AnalyticalLikelihood'
```

Listing A.1: QMLA Launch scipt

Figure	Exploration Strategy	N_E	N_P	Data
??	DemoHeuristicPGH	1000	3000	Nov_27/19_39
	DemoHeuristicNineEighths	1000	3000	Nov_27/19_40
	DemoHeuristicTimeList	1000	3000	Nov_27/19_42
	DemoHeuristicRandom	1000	3000	Nov_27/19_47
??	DemoProbesPlus	1000	3000	Nov_27/14_43
	DemoProbesZero	1000	3000	Nov_27/14_45
	DemoProbesTomographic	1000	3000	Nov_27/14_46
	DemoProbes	1000	3000	Nov_27/14_47
??	DemoProbesPlus	1000	3000	Nov_27/14_43
	DemoProbesZero	1000	3000	Nov_27/14_45
	DemoProbesTomographic	1000	3000	Nov_27/14_46
	DemoProbes	1000	3000	Nov_27/14_47
??	AnalyticalLikelihood	500	2000	Nov_16/14_28
??	DemoIsing	500	5000	Nov_18/13_56
??	DemoIsing	1000	5000	Nov_18/13_56
??	DemoIsing	1000	5000	Nov_18/13_56
??	IsingLatticeSet	1000	4000	Nov_19/12_04
	IsingLatticeSet	1000	4000	Nov_19/12_04
	IsingLatticeSet	1000	4000	Nov_19/12_04
??	IsingLatticeSet	1000	4000	Sep_30/22_40
	HeisenbergLatticeSet	1000	4000	Oct_22/20_45
	FermiHubbardLatticeSet	1000	4000	Oct_02/00_09

Table A.1: Implementation details for figures used in the main text. Continued in Table A.2.

Figure	Exploration Strategy	N_E	N_P	Data
Fig. 2.2	DemoBayesFactorsByFscore	500	2500	Dec_09/12_29
	DemoFractionalResourcesBayesFactorsByFscore	500	2500	Dec_09/12_31
	DemoBayesFactorsByFscore	1000	5000	Dec_09/12_33
	DemoBayesFactorsByFscoreEloGraphs	500	2500	Dec_09/12_32
Fig. 2.5	HeisenbergGeneticXYZ	500	2500	Dec_10/14_40
Fig. 2.6	HeisenbergGeneticXYZ	500	2500	Dec_10/14_40
	HeisenbergGeneticXYZ	500	2500	Dec_10/14_40
Fig. 2.7	HeisenbergGeneticXYZ	500	2500	Dec_10/16_12
	HeisenbergGeneticXYZ	500	2500	Dec_10/16_12
??	NVCentreExperimentalData	1000	3000	2019/Oct_02/18_01
	SimulatedExperimentNVCentre	1000	3000	2019/Oct_02/18_16
??	NVCentreExperimentalData	1000	3000	2019/Oct_02/18_01
??	SimulatedExperimentNVCentre	1000	3000	2019/Oct_02/18_16
??	SimulatedExperimentNVCentre	1000	3000	2019/Oct_02/18_16
	NVCentreExperimentalData	1000	3000	2019/Oct_02/18_01
??	NVCentreGenticAlgorithmPrelearnedParameters	2	5	Sep_09/12_00
	NVCentreGenticAlgorithmPrelearnedParameters	2	5	Sep_09/12_00
??	NVCentreGenticAlgorithmPrelearnedParameters	2	5	Sep_09/12_00
	NVCentreGenticAlgorithmPrelearnedParameters	2	5	Sep_09/12_00
??	NVCentreGenticAlgorithmPrelearnedParameters	2	5	Sep_08/23_58
??	NVCentreGenticAlgorithmPrelearnedParameters	2	5	Sep_08/23_58

Table A.2: [Continued from Table A.1] Implementation details for figures used in the main text.

B

FUNDAMENTALS

There are a number of concepts which are fundamental to any discussion of quantum mechanics (QM), but are likely to be known to most readers, and are therefore cumbersome to include in the main body of the thesis. We include them here for completeness[1].

B.1 LINEAR ALGEBRA

Here we review the language of linear algebra and summarise the basic mathematical techniques used throughout this thesis. We will briefly recall some definitions for reference.

- Notation

Definition of	Representation
Vector (or *ket*)	$\|\psi\rangle$
Dual Vector (or *bra*)	$\langle\psi\|$
Tensor Product	$\|\psi\rangle \otimes \|\phi\rangle$
Complex conjugate	$\|\psi^*\rangle$
Transpose	$\|\psi\rangle^T$
Adjoint	$\|\psi\rangle^\dagger = (\|\psi\rangle^*)^T$

Table B.1: Linear algebra definitions.

The dual vector of a vector (ket) $|\psi\rangle$ is given by $\langle\psi| = |\psi\rangle^\dagger$.

The *adjoint* of a matrix replaces each matrix element with its own complex conjugate, and then switches its columns with rows.

$$M^\dagger = \begin{pmatrix} M_{0,0} & M_{0,1} \\ M_{1,0} & M_{1,1} \end{pmatrix}^\dagger = \begin{pmatrix} M^*_{0,0} & M^*_{0,1} \\ M^*_{1,0} & M^*_{1,1} \end{pmatrix}^T = \begin{pmatrix} M^*_{0,0} & M^*_{1,0} \\ M^*_{0,1} & M^*_{1,1} \end{pmatrix} \tag{B.1}$$

1 Much of this description is reproduced from my undergraduate thesis [40].

The *inner product* of two vectors, $|\psi\rangle = \begin{pmatrix} \psi_1 \\ \psi_2 \\ \vdots \\ \psi_n \end{pmatrix}$ and $|\phi\rangle = \begin{pmatrix} \phi_1 \\ \phi_2 \\ \vdots \\ \phi_n \end{pmatrix}$ is given by

$$\langle\phi|\psi\rangle = (|\phi\rangle^\dagger)\,|\psi\rangle = (\phi_1^* \ \phi_2^* \ \dots \ \phi_n^*) \begin{pmatrix} \psi_1 \\ \psi_2 \\ \vdots \\ \psi_n \end{pmatrix} = \phi_1^*\psi_1 + \phi_2^*\psi_2 + \cdots + \phi_n^*\psi_n \tag{B.2}$$

$|\psi\rangle_i, |\phi\rangle_i$ are complex numbers, and therefore the above is simply a sum of products of complex numbers. The inner product is often called the *scalar product*, which is in general complex.

B.2 POSTULATES OF QUANTUM MECHANICS

There are numerous statements of the postulates of quantum mechanics. Each version of the statements aims to achieve the same foundation, so we endeavour to explain them in the simplest terms.

1 Every moving particle in a conservative force field has an associated wave-function, $|\psi\rangle$. From this wave-function, it is possible to determine all physical information about the system.

2 All particles have physical properties called observables (denoted Q). In order to determine a value, Q, for a particular observable, there is an associated *operator* $\hat{Q}$, which, when acting on the particles wavefunction, yields the value times the wavefunction. The observable Q is then the eigenvalue of the operator $\hat{Q}$.

$$\hat{Q}\,|\psi\rangle = q|\psi\rangle \tag{B.3}$$

3 Any such operator $\hat{Q}$ is Hermitian

$$\hat{Q}^\dagger = \hat{Q} \tag{B.4}$$

4 The set of eigenfunctions for any operator $\hat{Q}$ forms a complete set of linearly independent functions.

5 For a system with wavefunction $|\psi\rangle$, the expectation value of an observable Q with respect to an operator $\hat{Q}$ is denoted by $\langle q\rangle$ and is given by

$$\langle q\rangle = \langle\psi|\hat{Q}|\psi\rangle \tag{B.5}$$

6 The time evolution of $|\psi\rangle$ is given by the time dependent *Schrodinger Equation*

$$i\hbar\frac{\partial\psi}{\partial t} = \hat{H}\psi, \tag{B.6}$$

where $\hat{H}$ is the system's Hamiltonian.

Using these building blocks, we can begin to construct a language to describe quantum systems.

B.3 STATES

An orhthonormal basis consists of vectors of unit length which do not overlap, e.g. $|x_1\rangle = \begin{pmatrix}1\\0\end{pmatrix}, |x_2\rangle = \begin{pmatrix}0\\1\end{pmatrix} \Rightarrow \langle x_1|x_2\rangle = 0$. In general, if $\{|x\rangle\}$ are the eigenstates of a system, then the system can be written as some state vector, $|\psi\rangle$, in general a superposition over the basis-vectors:

$$|\psi\rangle = \sum_x a_x|x\rangle \tag{B.7a}$$

$$\text{subject to} \quad \sum_x |a_x|^2 = 1, \quad a_x \in \mathbb{C} \tag{B.7b}$$

The *state space* of a physical system (classical or quantum) is then the set of all possible states the system can exist in, i.e the set of all possible values for $|\psi\rangle$ such that Eq. (B.7b) are satisfied.

For example, photons can be polarised horizontally ($\leftrightarrow$) or vertically ($\updownarrow$); take those two conditions as observable states to define the eigenstates of a two-level system, so we can designate the photon as a qubit. Then we can map the two states to a 2-dimensional, x-y plane: a general vector on such a plane can be represented by a vector with coordinates $\begin{pmatrix}x\\y\end{pmatrix}$. These polarisations can then be thought of as standard basis vectors in linear algebra. Denote $\leftrightarrow$ as the eigenstate $|0\rangle$ and $\updownarrow$ as $|1\rangle$

$$|\leftrightarrow\rangle = |0\rangle = \begin{pmatrix}1\\0\end{pmatrix} \qquad \text{A unit vector along x-axis} \tag{B.8a}$$

$$|\updownarrow\rangle = |1\rangle = \begin{pmatrix}0\\1\end{pmatrix} \qquad \text{A unit vector along y-axis} \tag{B.8b}$$

Now, in relation to the concept of superposition, we can consider, for example, a photon in an even superposition of the vertical and horizontal polarisations, evenly splitting the two basis vectors. As such, we would require that, upon measurement, it is equally likely that the

photon will *collapse* into the polarised state along x as it is to collapse along y. That is, we want $\Pr(\updownarrow) = \Pr(\leftrightarrow)$ so assign equal modulus amplitudes to the two possibilities:

$$|\psi\rangle = a\,|\leftrightarrow\rangle + b\,|\updownarrow\rangle\,, \quad \text{with} \quad \Pr(\updownarrow) = \Pr(\leftrightarrow) \Rightarrow |a|^2 = |b|^2 \tag{B.9}$$

We consider here a particular case, due to the significance of the resultant basis, where $\leftrightarrow$-polarisation and $\updownarrow$-polarisation have real amplitudes $a, b \in \mathbb{R}$.

$$\begin{aligned} &\Rightarrow a = \pm b \quad \text{but also} \quad |a|^2 + |b|^2 = 1 \\ \Rightarrow \quad &a = \frac{1}{\sqrt{2}} \quad ; \quad b = \pm\frac{1}{\sqrt{2}} \\ &\Rightarrow |\psi\rangle = \frac{1}{\sqrt{2}}\,|\leftrightarrow\rangle \pm \frac{1}{\sqrt{2}}\,|\updownarrow\rangle \\ &\Rightarrow |\psi\rangle = \frac{1}{\sqrt{2}}\,|0\rangle \pm \frac{1}{\sqrt{2}}\,|1\rangle \end{aligned} \tag{B.10}$$

These particular superpositions are of significance:

$$|+\rangle = \frac{1}{\sqrt{2}}\,(|0\rangle + |1\rangle) \tag{B.11a}$$

$$|-\rangle = \frac{1}{\sqrt{2}}\,(|0\rangle - |1\rangle) \tag{B.11b}$$

This is called the Hadamard basis: it is an equally valid vector space as the standard basis which is spanned by $\begin{pmatrix}1\\0\end{pmatrix}, \begin{pmatrix}0\\1\end{pmatrix}$, as it is simply a rotation of the standard basis.

B.3.1 *Mulitpartite systems*

In reality, we often deal with systems of multiple particles, represented by multiple qubits. Mathematically, we consider the state vector of a system containing n qubits as being the tensor product of the n qubits' individual state vectors[2]. For instance, suppose a 2-qubit system, $|\psi\rangle$ consisting of two independent qubits $|\psi_A\rangle$ and $|\psi_B\rangle$:

$$|\psi\rangle = |\psi_A\rangle\,|\psi_B\rangle = |\psi_A\psi_B\rangle = |\psi_A\rangle \otimes |\psi_B\rangle \tag{B.12}$$

Consider first a simple system of 2 qubits. Measuring in the standard basis, these qubits will have to collapse in to one of the basis states $|0,0\rangle, |0,1\rangle, |1,0\rangle, |1,1\rangle$. Thus, for such a 2-qubit system, we have the general superposition

$$|\psi\rangle = \alpha_{0,0}|0,0\rangle + \alpha_{0,1}|0,1\rangle + \alpha_{1,0}|1,0\rangle + \alpha_{1,1}|1,1\rangle$$

2 We will later discuss entangled states, which can not be described thus.

where $\alpha_{i,j}$ is the amplitude for measuring the system as the state $|i,j\rangle$. This is perfectly analogous to a classical 2-bit system necessarily occupying one of the four possibilities $\{(0,0),(0,1),(1,0),(1,1)\}$.

Hence, for example, if we wanted to concoct a two-qubit system composed of one qubit in the state $|+\rangle$ and one in $|-\rangle$

$$\begin{aligned}
|\psi\rangle &= |+\rangle \otimes |-\rangle \\
|\psi\rangle &= \frac{1}{\sqrt{2}}\left(|0\rangle + |1\rangle\right) \otimes \frac{1}{\sqrt{2}}\left(|0\rangle - |1\rangle\right) \\
&= \frac{1}{2}\left[|00\rangle - |01\rangle + |10\rangle - |11\rangle\right] \\
&= \frac{1}{2}\left[\begin{pmatrix}1\\0\end{pmatrix} \otimes \begin{pmatrix}1\\0\end{pmatrix} - \begin{pmatrix}1\\0\end{pmatrix} \otimes \begin{pmatrix}0\\1\end{pmatrix} + \begin{pmatrix}0\\1\end{pmatrix} \otimes \begin{pmatrix}1\\0\end{pmatrix} - \begin{pmatrix}0\\1\end{pmatrix} \otimes \begin{pmatrix}0\\1\end{pmatrix}\right] \\
&= \frac{1}{2}\left[\begin{pmatrix}1\\0\\0\\0\end{pmatrix} - \begin{pmatrix}0\\1\\0\\0\end{pmatrix} + \begin{pmatrix}0\\0\\1\\0\end{pmatrix} - \begin{pmatrix}0\\0\\0\\1\end{pmatrix}\right]. \\
\Rightarrow |\psi\rangle &= \frac{1}{2}\begin{pmatrix}1\\-1\\-1\\1\end{pmatrix}
\end{aligned} \tag{B.13}$$

That is, the two qubit system – and indeed any two qubit system – is given by a linear combination of the four basis vectors

$$\{|00\rangle, |0,1\rangle, |10\rangle, |11\rangle\} = \left\{\begin{pmatrix}1\\0\\0\\0\end{pmatrix}, \begin{pmatrix}0\\1\\0\\0\end{pmatrix}, \begin{pmatrix}0\\0\\1\\0\end{pmatrix}, \begin{pmatrix}0\\0\\0\\1\end{pmatrix}\right\}. \tag{B.14}$$

We can notice that a single qubit system can be described by a linear combination of two basis vectors, and that a two qubit system requires four basis vectors to describe it. In general we can say that an n-qubit system is represented by a linear combination of 2^n basis vectors.

B.3.2 *Registers*

A *register* is generally the name given to an array of controllable quantum systems; here we invoke it to mean a system of multiple qubits, specifically a subset of the total number of

available qubits. For example, a register of ten qubits can be denoted $|x[10]\rangle$, and we can think of the system as a register of six qubits together with a register of three and another register of one qubit.

$$|x[10]\rangle = |x_1[6]\rangle \otimes |x_2[3]\rangle \otimes |x_3[1]\rangle$$

B.4 ENTANGLEMENT

Another unique property of quantum systems is that of *entanglement*: when two or more particles interact in such a way that their individual quantum states can not be described independent of the other particles. A quantum state then exists for the system as a whole instead. Mathematically, we consider such entangled states as those whose state can not be expressed as a tensor product of the states of the individual qubits it's composed of: they are dependent upon the other.

To understand what we mean by this dependence, consider a counter-example. Consider the Bell state,

$$|\Phi^+\rangle = \frac{1}{\sqrt{2}}\left(|00\rangle + |11\rangle\right), \tag{B.15}$$

if we measure this state, we expect that it will be observed in either eigenstate $|00\rangle$ or $|11\rangle$, with equal probability due to their amplitudes' equal magnitudes. The bases for this state are simply the standard bases, $|0\rangle$ and $|1\rangle$. Thus, according to our previous definition of systems of multiple qubits, we would say this state can be given as a combination of two states, like Eq. (B.12),

$$\begin{aligned} |\Phi^+\rangle &= |\psi_1\rangle \otimes |\psi_2\rangle \\ &= (a_1|0\rangle + b_1|1\rangle) \otimes (a_2|0\rangle + b_2|1\rangle) \\ &= a_1a_2|00\rangle + a_1b_2|01\rangle + b_1a_2|10\rangle + b_1b_2|11\rangle \end{aligned} \tag{B.16}$$

However we require $|\Phi^+\rangle = \frac{1}{\sqrt{2}}(|00\rangle + |11\rangle)$, which would imply $a_1b_2 = 0$ and $b_1a_2 = 0$. These imply that either $a_1 = 0$ or $b_2 = 0$, and also that $b_1 = 0$ or a_2=0, which are obviously invalid since we require that $a_1a_2 = b_1b_2 = \frac{1}{\sqrt{2}}$. Thus, we cannot express $|\Phi^+\rangle = |\psi_1\rangle \otimes |\psi_2\rangle$; this inability to separate the first and second qubits is what we term *entanglement*.

B.5 UNITARY TRANSFORMATIONS

A fundamental concept in quantum mechanics is that of performing transformations on states. *Quantum transformations*, or *quantum operators*, map a quantum state into a new state within the same Hilbert space. There are certain restrictions on a physically possible quantum transformation: in order that U is a valid transformation acting on some superposition $|\psi\rangle = a_1|\psi_1\rangle + a_2|\psi_2\rangle + \ldots a_k|\psi_k\rangle$, U must be linear

$$U(a_1|\psi_1\rangle + a_2|\psi_2\rangle + \ldots a_k|\psi_k\rangle) = a_1(U|\psi_1\rangle) + a_2(U|\psi_2\rangle) + \cdots + a_k(U|\psi_k\rangle). \tag{B.17}$$

To fulfil these properties, we require that U *preserve the inner product*:

$$\langle \psi_0 | U^\dagger U | \psi \rangle = \langle \psi_0 | \psi \rangle$$

That is, we require that any such transformation be *unitary*:

$$UU^\dagger = I \Rightarrow U^\dagger = U^{-1} \tag{B.18}$$

Unitarity is a sufficient condition to describe any valid quantum operation: any quantum transformation can be described by a unitary transformation, and any unitary transformation corresponds to a physically implementable quantum transformation.

Then, if U_1 is a unitary transformation that acts on the space $\mathcal{H}_1$ and U_2 acts on $\mathcal{H}_2$, the product of the two unitary transformations is also unitary. The tensor product $U_1 \otimes U_2$ acts on the space $\mathcal{H}_1 \otimes \mathcal{H}_2$. So, then, supposing a system of two separable qubits, $|\psi_1\rangle$ and $|\psi_2\rangle$ where we wish to act on $|\psi_1\rangle$ with operator U_1 and on $|\psi_2\rangle$ with U_2, we perform it as

$$(U_1 \otimes U_2)(|\psi_1\rangle \otimes |\psi_2\rangle) = (U_1 |\psi_1\rangle) \otimes (U_2 |\psi_2\rangle) \tag{B.19}$$

B.6 DIRAC NOTATION

In keeping with standard practice, we employ *Dirac notation* throughout this thesis. Vectors are denoted by *kets* of the form $|a\rangle$. For example, the standard basis is represented by,

$$\begin{aligned} |x\rangle = |0\rangle &= \begin{pmatrix} 1 \\ 0 \end{pmatrix} \\ |y\rangle = |1\rangle &= \begin{pmatrix} 0 \\ 1 \end{pmatrix} \end{aligned} \tag{B.20}$$

We saw in Table B.1 that for every such ket, $|\psi\rangle$, there exists a *dual vector*: its complex conjugate transpose, called the *bra* of such a vector, denoted $\langle \psi |$. That is,

$$\begin{aligned} \langle \psi |^\dagger &= |\psi\rangle \\ |\psi\rangle^\dagger &= \langle \psi | \end{aligned} \tag{B.21}$$

$$|\psi\rangle = \begin{pmatrix} \psi_1 \\ \psi_2 \\ \vdots \\ \psi_n \end{pmatrix} \Rightarrow \langle \psi | = \begin{pmatrix} \psi_1^* & \psi_2^* & \dots & \psi_n^* \end{pmatrix} \tag{B.22}$$

Then if we have two vectors $|\psi\rangle$ and $|\phi\rangle$, their *inner product* is given as $\langle\psi|\phi\rangle = \langle\phi|\psi\rangle$.

$$\begin{aligned} |\psi\rangle = \begin{pmatrix} \psi_1 \\ \psi_2 \\ \psi_3 \\ \vdots \\ \psi_n \end{pmatrix} \quad ; \quad |\phi\rangle = \begin{pmatrix} \phi_1 \\ \phi_2 \\ \phi_3 \\ \vdots \\ \phi_n \end{pmatrix} \\ \Rightarrow \langle\phi| = \begin{pmatrix} \phi_1^* & \phi_2^* & \phi_3^* & \dots & \phi_n^* \end{pmatrix} \\ \Rightarrow \langle\phi|\,|\psi\rangle = \begin{pmatrix} \phi_1^* & \phi_2^* & \phi_3^* & \dots & \phi_n^* \end{pmatrix} \begin{pmatrix} \psi_1 \\ \psi_2 \\ \psi_3 \\ \vdots \\ \psi_n \end{pmatrix} \\ \Rightarrow \langle\phi|\,|\psi\rangle = \phi_1^*\psi_1 + \phi_2^*\psi_2 + \phi_3^*\psi_3 + \cdots + \phi_n^*\psi_n \end{aligned} \tag{B.23}$$

Example B.6.1.

$$\begin{aligned} |\psi\rangle = \begin{pmatrix} 1 \\ 2 \\ 3 \end{pmatrix} \quad ; \quad |\phi\rangle = \begin{pmatrix} 4 \\ 5 \\ 6 \end{pmatrix} \\ \Rightarrow \langle\phi|\,|\psi\rangle = \begin{pmatrix} 4 & 5 & 6 \end{pmatrix} \begin{pmatrix} 1 \\ 2 \\ 3 \end{pmatrix} \\ = (4)(1) + (5)(2) + (6)(3) = 32 \end{aligned} \tag{B.24}$$

Similarly, their *outer product* is given as $|\phi\rangle\langle\psi|$. Multiplying a column vector by a row vector thus gives a matrix. Matrices generated by a outer products then define operators:

Example B.6.2.

$$\begin{pmatrix} 1 \\ 2 \end{pmatrix} \begin{pmatrix} 3 & 4 \end{pmatrix} = \begin{pmatrix} 3 & 4 \\ 6 & 8 \end{pmatrix} \tag{B.25}$$

Then we can say, for $|0\rangle = \begin{pmatrix} 1 \\ 0 \end{pmatrix}$ and $|1\rangle = \begin{pmatrix} 0 \\ 1 \end{pmatrix}$

$$|0\rangle\langle 0| = \begin{pmatrix} 1 & 0 \\ 0 & 0 \end{pmatrix} \tag{B.26a}$$

$$|0\rangle\langle 1| = \begin{pmatrix} 0 & 1 \\ 0 & 0 \end{pmatrix} \tag{B.26b}$$

$$|1\rangle\langle 0| = \begin{pmatrix} 0 & 0 \\ 1 & 0 \end{pmatrix} \tag{B.26c}$$

$$|1\rangle\langle 1| = \begin{pmatrix} 0 & 0 \\ 0 & 1 \end{pmatrix} \tag{B.26d}$$

And so any 2-dimensional linear transformation in the standard basis $|0\rangle, |1\rangle$ can be given as a sum

$$\begin{pmatrix} a & b \\ c & d \end{pmatrix} = a|0\rangle\langle 0| + b|0\rangle\langle 1| + c|1\rangle\langle 0| + d|1\rangle\langle 1| \tag{B.27}$$

This is a common method of representing operators as outer products of vectors. A transformation that *exchanges* a particle between two states, say $|0\rangle \leftrightarrow |1\rangle$ is given by the operation

$$\hat{Q} : \begin{cases} |0\rangle \to |1\rangle \\ |1\rangle \to |0\rangle \end{cases}$$

Which is equivalent to the outer product representation

$$\hat{Q} = |0\rangle\langle 1| + |1\rangle\langle 0|$$

For clarity, here we will prove this operation

Example B.6.3.

$$\begin{aligned} \hat{Q} &= |0\rangle\langle 1| + |1\rangle\langle 0| \\ &= \begin{pmatrix} 1 \\ 0 \end{pmatrix}\begin{pmatrix} 0 \\ 1 \end{pmatrix} + \begin{pmatrix} 0 \\ 1 \end{pmatrix}\begin{pmatrix} 1 \\ 0 \end{pmatrix} \\ &= \begin{pmatrix} 0 & 1 \\ 0 & 0 \end{pmatrix} + \begin{pmatrix} 0 & 0 \\ 1 & 0 \end{pmatrix} \\ &= \begin{pmatrix} 0 & 1 \\ 1 & 0 \end{pmatrix} \end{aligned}$$

So then, acting on $|0\rangle$ *and* $|1\rangle$ *gives*

$$\hat{Q}|0\rangle = \begin{pmatrix} 0 & 1 \\ 1 & 0 \end{pmatrix}\begin{pmatrix} 1 \\ 0 \end{pmatrix} = \begin{pmatrix} 0 \\ 1 \end{pmatrix} = |1\rangle$$

$$\hat{Q}\left|1\right\rangle = \begin{pmatrix} 0 & 1 \\ 1 & 0 \end{pmatrix} \begin{pmatrix} 0 \\ 1 \end{pmatrix} = \begin{pmatrix} 1 \\ 0 \end{pmatrix} = \left|0\right\rangle$$

To demonstrate how Dirac notation simplifies this:

$$\begin{aligned} \hat{Q}\left|0\right\rangle &= \left(\left|0\right\rangle\left\langle 1\right| + \left|1\right\rangle\left\langle 0\right|\right)\left|0\right\rangle \\ &= \left|0\right\rangle\left\langle 1\right|\left|0\right\rangle + \left|1\right\rangle\left\langle 0|0\right\rangle \\ &= \left|0\right\rangle\left\langle 1|0\right\rangle + \left|1\right\rangle\left\langle 0|0\right\rangle \end{aligned}$$

Then, since $\left|0\right\rangle$ and $\left|1\right\rangle$ are orthogonal basis, their inner product is 0 and the inner product of a vector with itself is 1, ($\left\langle 1|1\right\rangle = \left\langle 0|0\right\rangle = 1, \left\langle 0|1\right\rangle = \left\langle 1|0\right\rangle = 0$). So,

$$\begin{aligned} \hat{Q}\left|0\right\rangle &= \left|0\right\rangle(0) + \left|1\right\rangle(1) \\ \Rightarrow \hat{Q}\left|0\right\rangle &= \left|1\right\rangle \end{aligned} \tag{B.28}$$

And similarly for $\hat{Q}\left|1\right\rangle$. This simple example then shows why Dirac notation can significantly simplify calculations across quantum mechanics, compared to standard matrix and vector notation. To see this more clearly, we will examine a simple 2-qubit state under such operations. The method generalises to operating on two or more qubits generically: we can define any operator which acts on two qubits as a sum of outer products of the basis vectors $\left|00\right\rangle, \left|01\right\rangle, \left|10\right\rangle$ and $\left|11\right\rangle$. We can similarly define any operator which acts on an n qubit state as a linear combination of the 2^n basis states generated by the n qubits.

Example B.6.4. *To define a transformation that will exchange basis vectors $\left|00\right\rangle$ and $\left|11\right\rangle$, while leaving $\left|01\right\rangle$ and $\left|10\right\rangle$ unchanged (ie exchanging $\left|01\right\rangle \leftrightarrow \left|01\right\rangle, \left|10\right\rangle \leftrightarrow \left|10\right\rangle$) we define an operator*

$$\hat{Q} = \left|00\right\rangle\left\langle 11\right| + \left|11\right\rangle\left\langle 00\right| + \left|10\right\rangle\left\langle 10\right| + \left|01\right\rangle\left\langle 01\right| \tag{B.29}$$

Then, using matrix calculations this would require separately calculating the four outer products in the above sum and adding them to find a 4×4 matrix to represent $\hat{Q}$, which then acts on a state $\left|\psi\right\rangle$. Instead, consider first that $\left|\psi\right\rangle = \left|00\right\rangle$, ie one of the basis vectors our transformation is to change:

$$\hat{Q}\left|00\right\rangle = \left(\left|00\right\rangle\left\langle 11\right| + \left|11\right\rangle\left\langle 00\right| + \left|10\right\rangle\left\langle 10\right| + \left|01\right\rangle\left\langle 01\right|\right)\ \left|00\right\rangle \tag{B.30}$$

And as before, only the inner products of a vector with itself remains:

$$\begin{aligned} &= \left|00\right\rangle\left\langle 11\,|00\right\rangle + \left|11\right\rangle\left\langle 00\,|00\right\rangle + \left|10\right\rangle\left\langle 10\,|00\right\rangle + \left|01\right\rangle\left\langle 01\,|00\right\rangle \\ &= \left|00\right\rangle(0) + \left|11\right\rangle(1) + \left|10\right\rangle(0) + \left|01\right\rangle(0) \\ \Rightarrow &\hat{Q}\left|00\right\rangle = \left|11\right\rangle \end{aligned} \tag{B.31}$$

i.e the transformation has performed $\hat{Q} : |00\rangle \rightarrow |11\rangle$ *as expected. Then, if we apply the same transformation to a state which does not depend on one of the target states, eg,*

$$\begin{aligned} |\psi\rangle =& a\,|10\rangle + b\,|01\rangle \\ \hat{Q}\,|\psi\rangle =& \Big(|00\rangle\langle 11| + |11\rangle\langle 00| + |10\rangle\langle 10| + |01\rangle\langle 01| \Big)\Big(a\,|10\rangle + b\,|01\rangle \Big) \\ =& a\Big(|00\rangle\langle 11|10\rangle + |11\rangle\langle 00|10\rangle + |10\rangle\langle 10|10\rangle + |01\rangle\langle 01|10\rangle \Big) \\ &+ b\Big(|00\rangle\langle 11|01\rangle + |11\rangle\langle 00|01\rangle + |10\rangle\langle 10|01\rangle + |01\rangle\langle 01|01\rangle \Big) \end{aligned} \tag{B.32}$$

And since the inner product is a scalar, we can factor terms such as $\langle 11|10\rangle$ *to the beginning of expressions, eg* $|00\rangle\langle 11|\,|10\rangle = \langle 11\,|10\rangle\,|00\rangle$*, and we also know*

$$\begin{aligned} \langle 11|10\rangle = \langle 00|10\rangle = \langle 01|10\rangle = \langle 11|01\rangle = \langle 00|01\rangle = \langle 10|01\rangle = 0 \\ \langle 10|10\rangle = \langle 01|01\rangle = 1 \end{aligned} \tag{B.33}$$

We can express the above as

$$\begin{aligned} \hat{Q}\,|\psi\rangle =& a\Big((0)\,|00\rangle + (0)\,|11\rangle + (1)\,|10\rangle + (0)\,|01\rangle \Big) \\ &+ b\Big((0)\,|00\rangle + (0)\,|11\rangle + (0)\,|10\rangle + (1)|01\rangle \Big) \\ =& a\,|10\rangle\,| + b|01\rangle \\ =& |\psi\rangle \end{aligned} \tag{B.34}$$

Then it is clear that, when $|\psi\rangle$ *is a superposition of states unaffected by transformation* $\hat{Q}$*, then* $\hat{Q}\,|\psi\rangle = |\psi\rangle$*.*

This method generalises to systems with greater numbers of particles (qubits). If we briefly consider a 3 qubit system - and initialise all qubits in the standard basis state $|0\rangle$ - then the system is represented by $|000\rangle = |0\rangle \otimes |0\rangle \otimes |0\rangle = \begin{pmatrix} 0 \\ 1 \end{pmatrix} \otimes \begin{pmatrix} 0 \\ 1 \end{pmatrix} \otimes \begin{pmatrix} 0 \\ 1 \end{pmatrix}$. This quantity is an 8-row vector. To calculate the outer product $\langle 000|000\rangle$, we would be multiplying an 8-column bra $\langle 000|$ by an 8-row ket $|000\rangle$. Clearly then we will be working with 8×8 matrices, which will become quite difficult to maintain effectively and efficiently quite fast. As we move to systems of larger size, standard matrix multiplication becomes impractical for hand-written analysis, although of course remains tractable computationally up to $n \sim 10$ qubits. It is obvious that Dirac's bra/ket notation is a helpful, pathematically precise tool for QM.

C

EXAMPLE EXPLORATION STRATEGY RUN

Here we provide a complete example of how to run the Quantum Model Learning Agent (QMLA) framework, including how to implement a custom exploration strategy (ES), and generate/interpret analysis. Note: these examples are included in the QMLA documentation in a format that may be easier to follow – where possible, we recommend readers follow the Tutorial section of [41].

First, *fork* the QMLA codebase from [42] to a Github user account (referred to as username in Listing C.6). Now, we must download the code base and ensure it runs properly; these instructions are implemented via the command line[1].

The steps of preparing the codebase are

1. install redis;
2. create a virtual Python environment for installing QMLA dependencies without damaging other parts of the user's environment;
3. download the QMLA codebase from the forked Github repository;
4. install packages upon which QMLA depends.

```
# Install redis (database broker)
sudo apt update
sudo apt install redis-server

# make directory for QMLA
cd
mkdir qmla_test
cd qmla_test

# make Python virtual environment for QMLA
# note: change Python3.6 to desired version
sudo apt-get install python3.6-venv
python3.6 -m venv qmla-env
source qmla-env/bin/activate
```

1 Note: these instructions are tested for Linux and presumed to work on Mac, but untested on Windows. It is likely some of the underlying software (redis servers) can not be installed on Windows, so running on *Windows Subsystem for Linux* is advised.

```
# Download QMLA
git clone --depth 1 https://github.com/username/QMLA.git #
    REPLACE username

# Install dependencies
cd QMLA
pip install -r requirements.txt
```

Listing C.1: QMLA codebase setup language

Note there may be a problem with some packages in the requirements.txt arising from the attempt to install them all through a single call to pip install. Ensure these are all installed before proceeding.

When all of the requirements are installed, test that the framework runs. QMLA uses redis databases to store intermittent data: we must manually initialise the database. Run the following (note: here we list redis-4.0.8, but this must be corrected to reflect the version installed on the user's machine in the above setup section):

```
~/redis-4.0.8/src/redis-server
```

Listing C.2: Launch redis database

which should give something like Fig. C.1.

Figure C.1: Terminal running redis-server.

In a text editor, open qmla_test/QMLA/launch/local_launch.sh; here we will ensure that we are running the QHL algorithm, with 5 experiments and 20 particles, on the ES named TestInstall. Ensure the first few lines of local_launch.sh read:

```
#!/bin/bash

##### ------------------------------------------------ #####
# QMLA run configuration
##### ------------------------------------------------ #####
num_instances=2 # number of instances in run
run_qhl=0 # perform QHL on known (true) model
run_qhl_multi_model=0 # perform QHL for defined list of models
experiments=2 # number of experiments
particles=10 # number of particles
plot_level=5


##### ------------------------------------------------ #####
# Choose an exploration strategy
# This will determine how QMLA proceeds.
##### ------------------------------------------------ #####
exploration_strategy="TestInstall"
```

Listing C.3: local_launch script

Ensure the terminal running redis is kept active, and open a separate terminal window. We must activate the Python virtual environment configured for QMLA, which we set up in Listing C.6. Then, we navigate to the QMLA directory, and launch:

```
# activate the QMLA Python virtual environment
source qmla_test/qmla-env/bin/activate

# move to the QMLA directory
cd qmla_test/QMLA
# Run QMLA
cd launch
./local_launch.sh
```

Listing C.4: Launch QMLA

There may be numerous warnings, but they should not affect whether QMLA has succeeded; QMLA will raise any significant error. Assuming the run has completed successfully, QMLA stores the run's results in a subdirectory named by the date and time it was started. For example, if the run was initialised on January 1st at 01:23, navigate to the corresponding directory by

```
cd results/Jan_01/01_23
```

Listing C.5: QMLA results directory

For now it is sufficient to notice that the code has run successfully: it should have generated (in results/Jan_01/01_23) files like storage_001.p and results_001.p.

C.1 CUSTOM EXPLORATION STRATEGY

Next, we design a basic ES, for the purpose of demonstrating how to run the algorithm. ESs are placed in the directory qmla/exploration_strategies. To make a new one, navigate to the exploration strategies directory, make a new subdirectory, and copy the template file.

```
cd ~/qmla_test/QMLA/exploration_strategies/
mkdir custom_es

# Copy template file into example
cp template.py custom_es/example.py
cd custom_es
```

Listing C.6: QMLA codebase setup

Ensure QMLA will know where to find the ES by importing everything from the custom ES directory into to the main exploration_strategy module. Then, in the custom_es directory, make a file called __init__.py which imports the new ES from the example.py file. To add any further ESs inside the directory custom_es, include them in the custom __init__.py, and they will automatically be available to QMLA.

```
# inside qmla/exploration_strategies/custom_es
#   __init__.py
from qmla.exploration_strategies.custom_es.example import *

# inside qmla/exploration_strategies , add to the existing
# __init__.py
from qmla.exploration_strategies.custom_es import *
```

Listing C.7: Providing custom exploration strategy to QMLA

Now, change the structure (and name) of the ES inside custom_es/example.py. Say we wish to target the true model

$$\begin{aligned} \vec{\alpha} &= (\alpha_{1,2} \quad \alpha_{2,3} \quad \alpha_{3,4}) \\ \vec{T} &= \begin{pmatrix} \hat{\sigma}_z^1 \otimes \hat{\sigma}_z^2 \\ \hat{\sigma}_z^2 \otimes \hat{\sigma}_z^3 \\ \hat{\sigma}_z^3 \otimes \hat{\sigma}_z^4 \end{pmatrix} \\ \implies \hat{H}_0 &= \hat{\sigma}_z^{(1,2)} \hat{\sigma}_z^{(2,3)} \hat{\sigma}_z^{(3,4)} \end{aligned} \tag{C.1}$$

QMLA interprets models as strings, where terms are separated by $+$, and parameters are implicit. So the target model in Eq. (C.1) will be given by

pauliSet_1J2_zJz_d4+pauliSet_2J3_zJz_d4+pauliSet_3J4_zJz_d4.

Adapting the template ES slightly, we can define a model generation strategy with a small number of hard coded candidate models introduced at the first branch of the exploration tree. We will also set the parameters of the terms which are present in $\hat{H}_0$, as well as the range in which to search parameters. Keeping the imports at the top of the example.py, rewrite the ES as:

```
class ExampleBasic(
    exploration_strategy.ExplorationStrategy
):

    def __init__(
        self,
        exploration_rules,
        true_model=None,
        **kwargs
    ):
        self.true_model = 'pauliSet_1J2_zJz_d4+
            pauliSet_2J3_zJz_d4+pauliSet_3J4_zJz_d4'
        super().__init__(
            exploration_rules=exploration_rules,
            true_model=self.true_model,
            **kwargs
        )

        self.initial_models = None
        self.true_model_terms_params = {
            'pauliSet_1J2_zJz_d4' : 2.5,
```

```
            'pauliSet_2J3_zJz_d4' : 7.5,
            'pauliSet_3J4_zJz_d4' : 3.5,
        }
        self.tree_completed_initially = True
        self.min_param = 0
        self.max_param = 10

    def generate_models(self, **kwargs):

        self.log_print(["Generating models; spawn step {}".format
            (self.spawn_step)])
        if self.spawn_step == 0:
            # chains up to 4 sites
            new_models = [
                'pauliSet_1J2_zJz_d4',
                'pauliSet_1J2_zJz_d4+pauliSet_2J3_zJz_d4',
                'pauliSet_1J2_zJz_d4+pauliSet_2J3_zJz_d4+
                    pauliSet_3J4_zJz_d4',
            ]
            self.spawn_stage.append('Complete')

        return new_models
```

Listing C.8: ExampleBasic exploration strategy.

To run[2] the example ES for a meaningful test, return to the local_launch of Listing C.3, but change some of the settings:

```
particles=2000
experiments=500
run_qhl=1
exploration_strategy=ExampleBasic
```

Listing C.9: local_launch configuration for QHL.

Run locally again as in Listing C.4; then move to the results directory as in Listing C.5.

2 Note this will take up to 15 minutes to run. This can be reduced by lowering the values of particles, experiments, which is sufficient for testing but note that the outcomes will be less effective than those presented in the figures of this section.

C.2 ANALYSIS

QMLA stores results and generates plots over the entire range of the algorithm[3], i.e. the run, instance and models. The depth of analysis performed automatically is set by the user control plot_level in local_launch.sh; for plot_level=1, only the most crucial figures are generated, while plot_level=6 generates plots for every individual model considered. For model searches across large model spaces and/or considering many candidates, excessive plotting can cause considerable slow-down, so users should be careful to generate plots only to the degree they will be useful. Next we show some examples of the available plots.

C.2.1 *Model analysis*

We have just run quantum Hamiltonian learning (QHL) for the model in Eq. (C.1) for a single instance, using a reasonable number of particles and experiments, so we expect to have trained the model well. Instance-level results are stored (e.g. for the instance with qmla_id=1) in Jan_01/01_23/instances/qmla_1. Individual models' insights can be found in model_training, e.g. the model's learning_summary Fig. C.2a, and dynamics in Fig. C.2b.

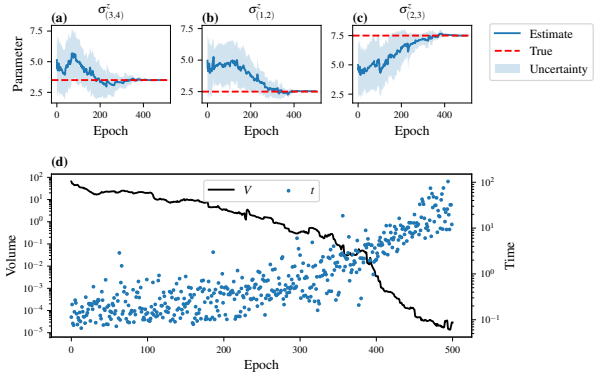

(a)

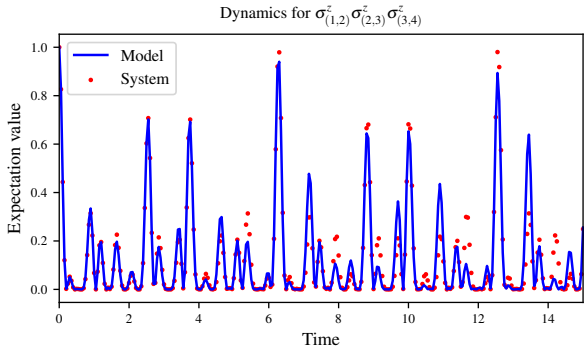

(b)

Figure C.2: Model analysis plots, stored in (for example) Jan_01/01_23/instances/qmla_1/model_training. **a** learning_summary_1. Displays the outcome of QHL for the given model: Subfigures (a)-(c) show the estimates of the parameters; (d) shows the total parameterisation volume against experiments trained upon, along with the evolution times used for those experiments. **(b)** dynamics_1 The model's attempt at reproducing dynamics from $\hat{H}_0$.

3 Recall that a single implementation of QMLA is called an instance, while a series of instances – which share the same target model – is called the run.

C.2.2 *Instance analysis*

Now we can run the full QMLA algorithm, i.e. train several models and determine the most suitable. QMLA will call the generate_models method of the ExampleBasic ES, set in Listing C.8, which tells QMLA to construct three models on the first branch, then terminate the search. Here we need to train and compare all models so it takes considerably longer to run: for the purpose of testing, we reduce the resources so the entire algorithm runs in about 15 minutes. Some applications will require significantly more resources to learn effectively. In realistic cases, these processes are run in parallel, as we will cover in Appendix C.3.

Reconfigure a subset of the settings in the local_launch.sh script (Listing C.3) and run it again:

```
experiments=250
particles=1000
run_qhl=0
exploration_strategy=ExampleBasic
```

Listing C.10: local_launch configuration for QMLA.

In the corresponding results directory, navigate to instances/qmla_1, where instance level analysis are available.

```
cd results/Jan_01/01_23/instances/qmla_1
```

Listing C.11: Navigating to instance results.

Figures of interest here show the composition of the models (Fig. C.3a), as well as the Bayes factors between candidates (Fig. C.3b). Individual model comparisons – i.e. Bayes factor (BF) – are shown in Fig. C.3c, with the dynamics of all candidates shown in Fig. C.4c. The probes used during the training of all candidates are also plotted (Fig. C.3e).

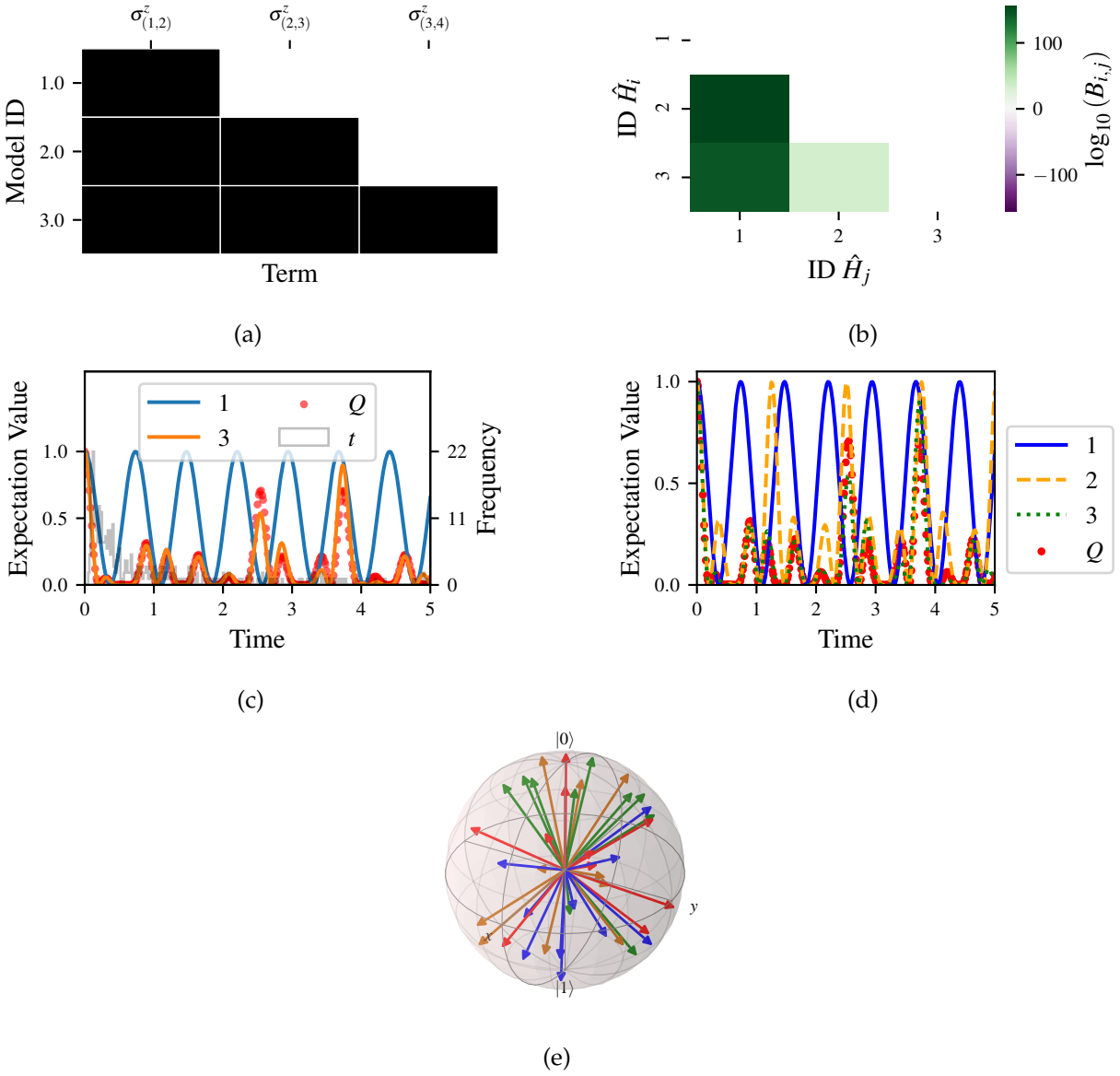

Figure C.3: QMLA plots; found within instance directory e.g. Jan_01/01_23/instances/qmla_1, and its subdirectories. **(a)** composition_of_models: constituent terms of all considered models, indexed by their model IDs. Here model 3 is $\hat{H}_0$. **(b)** bayes_factors: Bayes factor (BF) comparisons between all models. BFs are read as $B_{i,j}$ where i is the model with lower ID, e.g. $B_{1,2}$ rather than $B_{2,1}$. Thus $B_{ij} > 0$ (< 0) indicates $\hat{H}_i$ ($\hat{H}_j$), i.e. the model on the y-axis (x-axis) is the stronger model. **(c)** comparisons/BF_1_3: direct comparison between models with IDs 1 and 3, showing their reproduction of the system dynamics (red dots, Q), as well as the times (experiments) against which the BF was calculated. **(d)** branches/dynamics_branch_1: dynamics of all models considered on the branch compared with system dynamics (red dots, Q). **(e)** probes_bloch_sphere: probes used for training models in this instance (only showing 1-qubit versions).

C.2.3 *Run analysis*

Considering a number of instances together is a *run*. In general, this is the level of analysis of most interest: an individual instance is liable to errors due to the probabilistic nature of the model training and generation subroutines. On average, however, we expect those elements to perform well, so across a significant number of instances, we expect the average outcomes to be meaningful.

Each results directory has an analyse.sh script to generate plots at the run level.

```
cd results/Jan_01/01_23
./analyse.sh
```

Listing C.12: Analysing QMLA run.

Run level analysis are held in the main results directory and several sub-directories created by the analyse script. Here, we recommend running a number of instances with very few resources so that the test finishes quickly[4]. The results will therefore be meaningless, but allow fo elucidation of the resultant plots. First, reconfigure some settings of Listing C.3 and launch again.

```
num_instances=10
experiments=20
particles=100
run_qhl=0
exploration_strategy=ExampleBasic
```

Listing C.13: local_launch configuration for QMLA run.

Some of the generated analysis are shown in Figs. C.4 to C.5. The number of instances for which each model was deemed champion, i.e. their *win rates* are given in Fig. C.4a. The *top models*, i.e. those with highest win rates, analysed further: the average parameter estimation progression for $\hat{H}_0$ – including only the instances where $\hat{H}_0$ was deemed champion – are shown in Fig. C.4b. Irrespecitve of the champion models, the rate with which each term is found in the champion model ($\hat{t} \in \hat{H}'$) indicates the likelihood that the term is really present; these rates – along with the parameter values learned – are shown in Fig. C.4c. The champion model from each instance can attempt to reproduce system dynamics: we group together these reproductions for each model in Fig. C.5.

4 This run will take about ten minutes

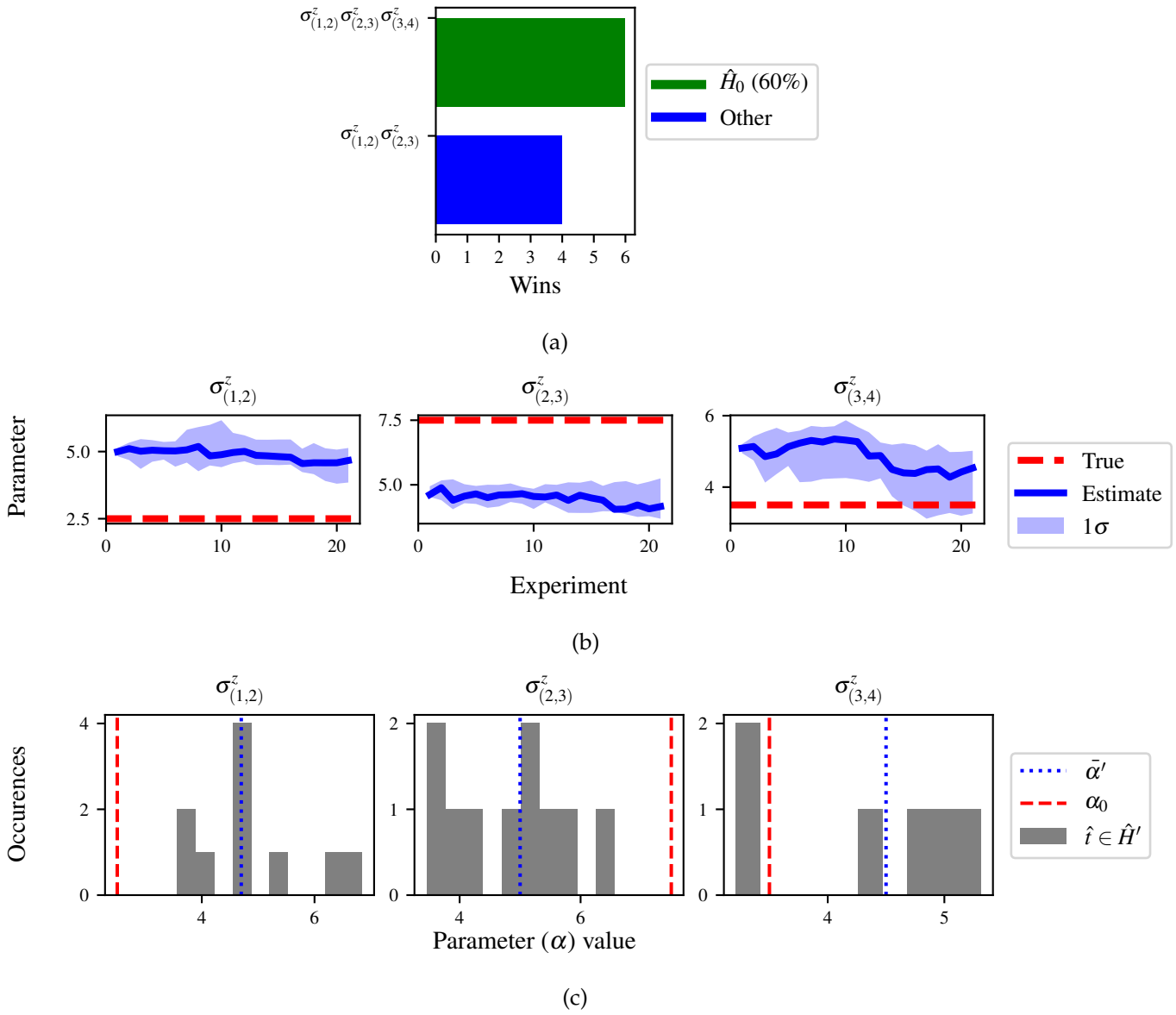

Figure C.4: QMLA run plots; found within run directory e.g. Jan_01/01_23/. **(a)** performance/model_wins: number of instance wins achieved by each model. **(b)** champion_models/params_params_pauliSet_1J2_zJz_d4+pauliSet_2J3_zJz_d4+pauliSet_3J4_zJz_d4: parameter estimation progression for the true model , only for the instances where it was deemed champion. **(c)** champion_models/terms_and_params: histogram of parameter values found for each term which appears in any champion model, with the true parameter (α_0) in red and the median learned parameter ($\bar{\alpha}'$) in blue.

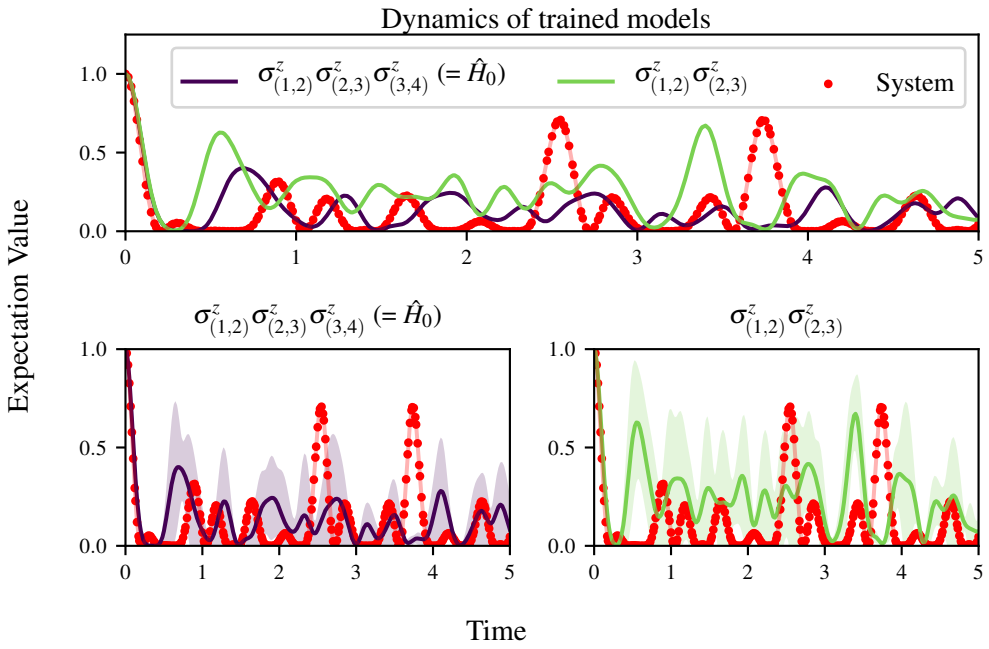

Figure C.5: Run plot performace/dynamics: median dynamics of the champion models. The models which won most instances are shown together in the top panel, and individually in the lower panels. The median dynamics from the models' learnings in its winning instances are shown, with the shaded region indicating the 66% confidence region.

C.3 PARALLEL IMPLEMENTATION

We provide utility to run QMLA on parallel processes. Individual models' training can run in parallel, as well as the calculation of BF between models. The provided script is designed for portable batch system (PBS) job scheduler running on a compute cluster. It will require a few adjustments to match the system being used. Overall, though, it has mostly a similar structure as the local_launch.sh script used above.

QMLA must be downloaded on the compute cluster as in Listing C.6; this can be a new fork of the repository, though it is sensible to test installation locally as described in this chapter so far, then *push* that version, including the new ES, to Github, and cloning the latest version. It is again advisable to create a Python virtual environment in order to isolate QMLA and its dependencies[5]. Open the parallel launch script, QMLA/launch/parallel_launch.sh, and prepare the first few lines as

```
#!/bin/bash
```

5 Indeed it is sensible to do this for any Python development project.

```
##### ---------------------------------------------- #####
# QMLA run configuration
##### ---------------------------------------------- #####
num_instances=10 # number of \glspl{instance} in run
run_qhl=0 # perform QHL on known (true) model
run_qhl_multi_model=0 # perform QHL for defined list of models
experiments=250
particles=1000
plot_level=5


##### ---------------------------------------------- #####
# Choose an exploration strategy
# This will determine how QMLA proceeds.
##### ---------------------------------------------- #####
exploration_strategy="ExampleBasic"
```

Listing C.14: parallel_launch script

When submitting jobs to schedulers like PBS, we must specify the time required, so that it can determine a fair distribution of resources among users. We must therefore *estimate* the time it will take for an instance to complete: clearly this is strongly dependent on the numbers of experiments (N_e) and particles (N_p), and the number of models which must be trained. QMLA attempts to determine a reasonable time to request based on the max_num_models_by_shape attribute of the ES, by calling QMLA/scripts/time_required_calculation.py. In practice, this can be difficult to set perfectly, so the timing_insurance_factor attribute of the ES can be used to correct for heavily over- or under-estimated time requests. Instances are run in parallel, and each instance trains/compares models in parallel. The number of processes to request, N_c for each instance is set as num_processes_to_parallelise_over in the ES. Then, if there are N_r instances in the run, we will be requesting the job scheduler to admit N_r distinct jobs, each requiring N_c processes, for the time specified.

The parallel_launch script works together with launch/run_single_qmla_instance.sh, though note a number of steps in the latter are configured to the cluster and may need to be adapted. In particular, the first command is used to load the redis utility, and later lines are used to initialise a redis server. These commands will probably not work with most machines, so must be configured to achieve those steps.

```
module load tools/redis-4.0.8

...
```

```
SERVER_HOST=$(head -1 "$PBS_NODEFILE")
let REDIS_PORT="6300 + $QMLA_ID"

cd $LIBRARY_DIR
redis-server RedisDatabaseConfig.conf --protected-mode no --port
    $REDIS_PORT &
redis-cli -p $REDIS_PORT flushall
```

Listing C.15: run_single_qmla_instance script

When the modifications are finished, QMLA can be launched in parallel similarly to the local version:

```
source qmla_test/qmla-env/bin/activate

cd qmla_test/QMLA/launch
./parallel_launch.sh
```

Listing C.16: run_single_qmla_instance script

Jobs are likely to queue for some time, depending on the demands on the job scheduler. When all jobs have finished, results are stored as in the local case, in QMLA/launch/results/-Jan_01/01_23, where analyse.sh can be used to generate a series of automatic analyses.

C.4 CUSTOMISING EXPLORATION STRATEGYS

User interaction with the QMLA codebase should be achieveable primarily through the exploration strategy (ES) framework. Throughout the algorithm(s) available, QMLA calls upon the ES before determining how to proceed. The usual mechanism through which the actions of QMLA are directed, is to set attributes of the ES class: the complete set of influential attributes are available at [41].

QMLA directly uses several methods of the ES class, all of which can be overwritten in the course of customising an ES. Most such methods need not be replaced, however, with the exception of generate_models, which is the most important aspect of any ES: it determines which models are built and tested by QMLA. This method allows the user to impose any logic desired in constructing models; it is called after the completion of every branch of the exploration tree on the ES.

C.4.1 *Greedy search*

A first non-trivial ES is to build models greedily from a set of *primitive* terms, $\mathcal{T} = \{\hat{t}\}$. New models are constructed by combining the previous branch champion with each of the remaining, unused terms. The process is repeated until no terms remain.

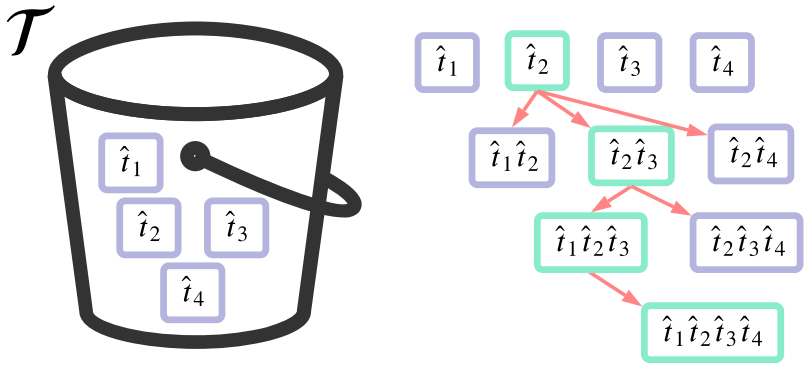

Figure C.6: Greedy search mechanism. **Left**, a set of primitive terms, $\mathcal{T}$, are defined in advance. **Right**, models are constructed from $\mathcal{T}$. On the first branch, the primitve terms alone constitute models. Thereafter, the strongest model (marked in green) from the previous branch is combined with all the unused terms.

We can compose an ES using these rules, say for

$$\mathcal{T} = \left\{\hat{\sigma}_x^1,\ \hat{\sigma}_y^1,\ \hat{\sigma}_x^1 \otimes \hat{\sigma}_x^2,\ \hat{\sigma}_y^1 \otimes \hat{\sigma}_y^2\right\}$$

as follows. Note the termination criteria must work in conjunction with the model generation routine. Users can overwrite the method check_tree_completed for custom logic, although a straightforward mechanism is to use the spawn_stage attribute of the ES class: when the final element of this list is Complete, QMLA will terminate the search by default. Also note that the default termination test checks whether the number of branches (spawn_step) exceeds the limit max_spawn_depth, which must be set artifically high to avoid ceasing the search too early, if relying solely on spawn_stage. Here we demonstrate how to impose custom logic to terminate the seach also.

```
class ExampleGreedySearch(
    exploration_strategy.ExplorationStrategy
):
    r"""
    From a fixed set of terms, construct models iteratively,
```

```
    greedily adding all unused terms to separate models at each
       call to the generate_models.

    """

    def __init__(
        self,
        exploration_rules,
        **kwargs
    ):

        super().__init__(
            exploration_rules=exploration_rules,
            **kwargs
        )
        self.true_model = 'pauliSet_1_x_d3+pauliSet_1J2_yJy_d3+
           pauliSet_1J2J3_zJzJz_d3'
        self.initial_models = None
        self.available_terms = [
            'pauliSet_1_x_d3', 'pauliSet_1_y_d3',
            'pauliSet_1J2_xJx_d3', 'pauliSet_1J2_yJy_d3'
        ]
        self.branch_champions = []
        self.prune_completed_initially = True
        self.check_champion_reducibility = False

    def generate_models(
        self,
        model_list,
        **kwargs
    ):
        self.log_print([
            "Generating models in tiered greedy search at spawn
               step {}.".format(
                 self.spawn_step,
            )
        ])
        try:
            previous_branch_champ = model_list[0]
            self.branch_champions.append(previous_branch_champ)
```

```
        except:
            previous_branch_champ = ""

        if self.spawn_step == 0 :
            new_models = self.available_terms
        else:
            new_models = greedy_add(
                current_model = previous_branch_champ,
                terms = self.available_terms
            )

        if len(new_models) == 0:
            # Greedy search has exhausted the available models;
            # send back the list of branch champions and
               terminate search.
            new_models = self.branch_champions
            self.spawn_stage.append('Complete')

        return new_models

def greedy_add(
    current_model,
    terms,
):
    r"""
    Combines given model with all terms from a set.

    Determines which terms are not yet present in the model,
    and adds them each separately to the current model.

    :param str current_model: base model
    :param list terms: list of strings of terms which are to be
       added greedily.
    """


    try:
        present_terms = current_model.split('+')
    except:
        present_terms = []
    nonpresent_terms = list(set(terms) - set(present_terms))
```

```
    term_sets = [
        present_terms+[t] for t in nonpresent_terms
    ]

    new_models = ["+".join(term_set) for term_set in term_sets]

    return new_models
```

Listing C.17: ExampleGreedySearch exploration stategy

This run can be implemented locally or in parallel as described above[6], and analysed as in Listing C.12, generating figures in accordance with the plot_level set by the user in the launch script. Outputs can again be found in the instances subdirectory, including a map of the models generated, as well as the branches they reside on, and the BFs between candidates, Fig. C.7.

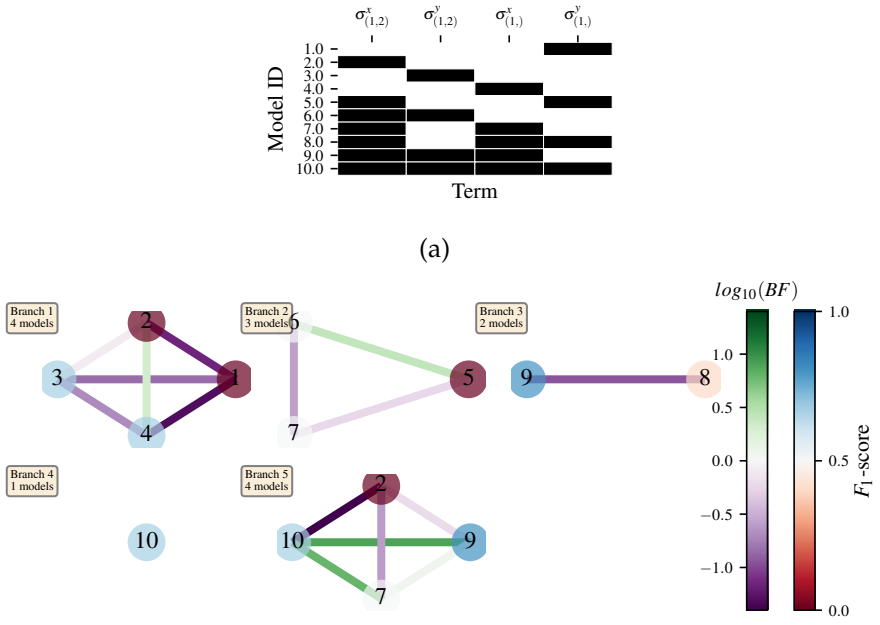

(a)

(b)

Figure C.7: Greedy exploration strategy. **(a)**, composition_of_models. **b**, graphs_of_branches_ExampleGreedySearch: shows which models reside on each branches of the exploration tree. Models are coloured by their F_1-score, and edges represent the BF between models. The first four branches are equivalent to those in Fig. C.6 , while the final branch considers the set of branch champions, in order to determine the overall champion.

6 We advise reducing plot_level to 3 to avoid excessive/slow figure generation.

C.4.2 *Tiered greedy search*

We provide one final example of a non-trivial ES: tiered greedy search. Similar to the idea of Appendix C.4.1, except terms are introduced hierarchically: sets of terms $\mathcal{T}_1, \mathcal{T}_2, \ldots \mathcal{T}_n$ are each examined greedily, where the overall strongest model of one tier forms the seed model for the subsequent tier. This is depicted in the main text in **??**. A corresponding ES is given as follows.

```
class ExampleGreedySearchTiered(
    exploration_strategy.ExplorationStrategy
):
    r"""
    Greedy search in tiers.

    Terms are batched together in tiers;
    tiers are searched greedily;
    a single tier champion is elevated to the subsequent tier.

    """

    def __init__(
        self,
        exploration_rules,
        **kwargs
    ):
        super().__init__(
            exploration_rules=exploration_rules,
            **kwargs
        )
        self.true_model = 'pauliSet_1_x_d3+pauliSet_1J2_yJy_d3+
           pauliSet_1J2J3_zJzJz_d3'
        self.initial_models = None
        self.term_tiers = {
            1 : ['pauliSet_1_x_d3', 'pauliSet_1_y_d3', '
               pauliSet_1_z_d3' ],
            2 : ['pauliSet_1J2_xJx_d3', 'pauliSet_1J2_yJy_d3', '
               pauliSet_1J2_zJz_d3'],
            3 : ['pauliSet_1J2J3_xJxJx_d3', '
               pauliSet_1J2J3_yJyJy_d3', 'pauliSet_1J2J3_zJzJz_d3
               '],
```

```
        }
        self.tier = 1
        self.max_tier = max(self.term_tiers)
        self.tier_branch_champs = {k : [] for k in self.
            term_tiers}
        self.tier_champs = {}
        self.prune_completed_initially = True
        self.check_champion_reducibility = True

    def generate_models(
        self,
        model_list,
        **kwargs
    ):
        self.log_print([
            "Generating models in tiered greedy search at spawn
                step {}.".format(
                self.spawn_step,
            )
        ])

        if self.spawn_stage[-1] is None:
            try:
                previous_branch_champ = model_list[0]
                self.tier_branch_champs[self.tier].append(
                    previous_branch_champ)
            except:
                previous_branch_champ = None

        elif "getting_tier_champ" in self.spawn_stage[-1]:
            previous_branch_champ = model_list[0]
            self.log_print([
                "Tier champ for {} is {}".format(self.tier,
                    model_list[0])
            ])
            self.tier_champs[self.tier] = model_list[0]
            self.tier += 1
            self.log_print(["Tier now = ", self.tier])
            self.spawn_stage.append(None) # normal processing
```

```
            if self.tier > self.max_tier:
                self.log_print(["Completed tree for ES"])
                self.spawn_stage.append('Complete')
                return list(self.tier_champs.values())
        else:
            self.log_print([
                "Spawn stage:", self.spawn_stage
            ])

        new_models = greedy_add(
            current_model = previous_branch_champ,
            terms = self.term_tiers[self.tier]
        )
        self.log_print([
            "tiered search new_models=", new_models
        ])

        if len(new_models) == 0:
            # no models left to find - get champions of branches
               from this tier
            new_models = self.tier_branch_champs[self.tier]
            self.log_print([
                "tier champions: {}".format(new_models)
            ])
            self.spawn_stage.append("getting_tier_champ_{}".
               format(self.tier))
        return new_models

    def check_tree_completed(
        self,
        spawn_step,
        **kwargs
    ):
        r"""
        QMLA asks the exploration tree whether it has finished
           growing;
        the exploration tree queries the exploration strategy
           through this method
        """
        if self.tree_completed_initially:
```

```
            return True
        elif self.spawn_stage[-1] == "Complete":
            return True
        else:
            return False


def greedy_add(
    current_model,
    terms,
):
    r"""
    Combines given model with all terms from a set.

    Determines which terms are not yet present in the model,
    and adds them each separately to the current model.

    :param str current_model: base model
    :param list terms: list of strings of terms which are to be
       added greedily.
    """

    try:
        present_terms = current_model.split('+')
    except:
        present_terms = []
    nonpresent_terms = list(set(terms) - set(present_terms))

    term_sets = [
        present_terms+[t] for t in nonpresent_terms
    ]

    new_models = ["+".join(term_set) for term_set in term_sets]

    return new_models
```

Listing C.18: ExampleGreedySearchTiered exploration stategy

with corresponding results in Fig. C.8.

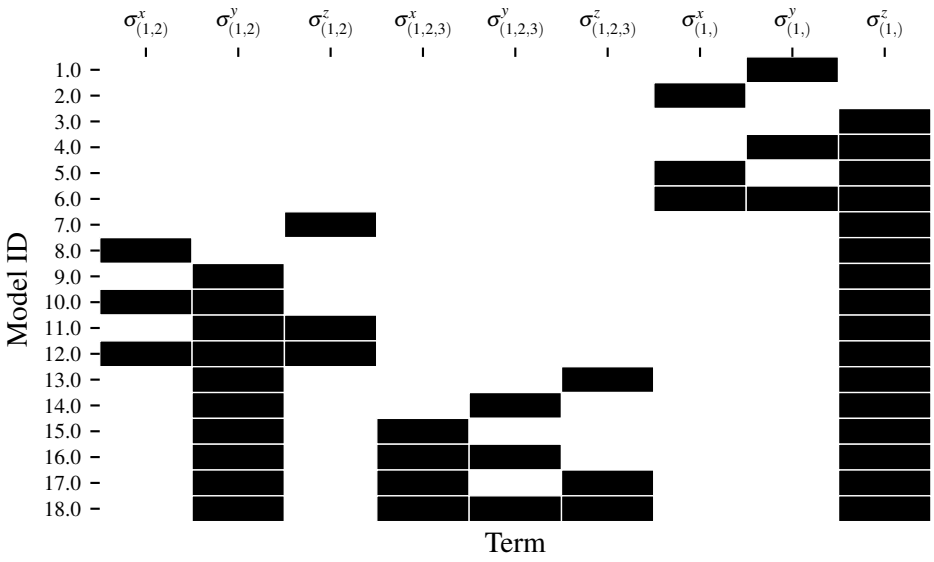

(a)

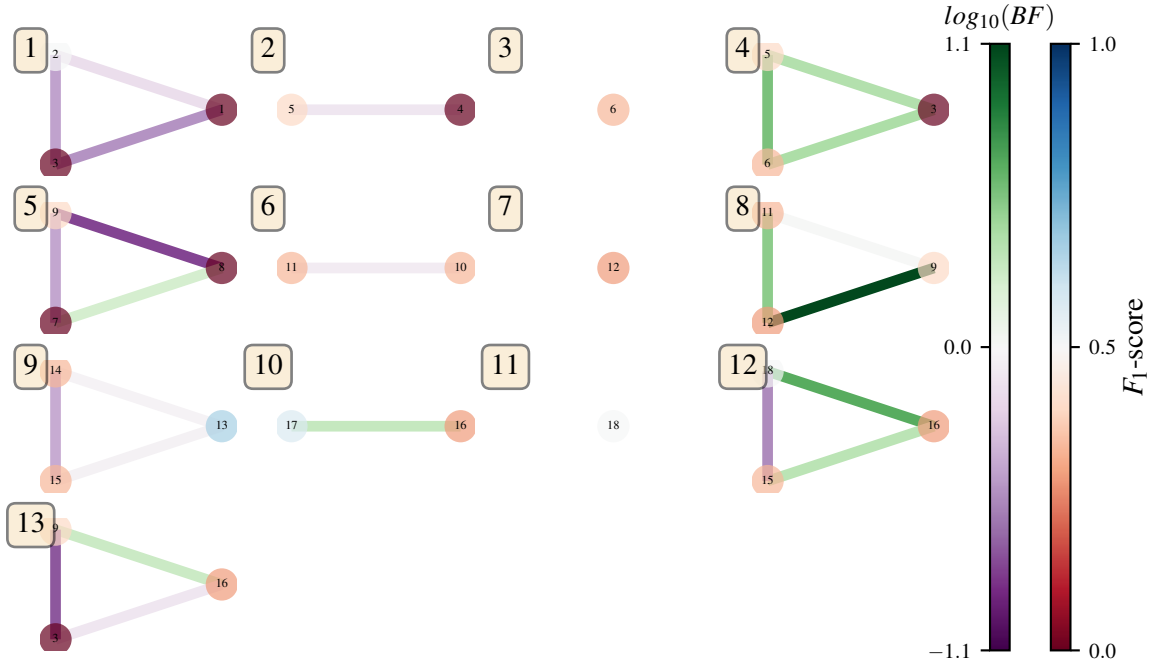

(b)

Figure C.8: Tiered greedy exploration strategy. **(a)**, composition_of_models. **b**, graphs_of_branches_ExampleGreedySearchTiered: shows which models reside on each branches of the exploration tree. Models are coloured by their F_1-score, and edges represent the BF between models. In each tier, three branches greedily add terms, and a fourth branch considers the champions of the first three branches in order to nominate a tier champion. The final branch consists only of the tier champions, to nominate the global champion, $\hat{H}'$.

BIBLIOGRAPHY

[1] The Difference Between AI and Machine Learning, Jan 2021. [Online; accessed 7. Jan. 2021].

[2] Warren S McCulloch and Walter Pitts. A logical calculus of the ideas immanent in nervous activity. *The bulletin of mathematical biophysics*, 5(4):115–133, 1943.

[3] Alan M Turing. Computing machinery and intelligence. In *Parsing the turing test*, pages 23–65. Springer, 2009.

[4] Stuart Russell and Peter Norvig. Artificial intelligence: a modern approach. 2002.

[5] Fabian Pedregosa, Gaël Varoquaux, Alexandre Gramfort, Vincent Michel, Bertrand Thirion, Olivier Grisel, Mathieu Blondel, Peter Prettenhofer, Ron Weiss, Vincent Dubourg, et al. Scikit-learn: Machine learning in python. *the Journal of machine Learning research*, 12:2825–2830, 2011.

[6] Martín Abadi, Paul Barham, Jianmin Chen, Zhifeng Chen, Andy Davis, Jeffrey Dean, Matthieu Devin, Sanjay Ghemawat, Geoffrey Irving, Michael Isard, et al. Tensorflow: A system for large-scale machine learning. In *12th {USENIX} symposium on operating systems design and implementation ({OSDI} 16)*, pages 265–283, 2016.

[7] Adam Paszke, Sam Gross, Francisco Massa, Adam Lerer, James Bradbury, Gregory Chanan, Trevor Killeen, Zeming Lin, Natalia Gimelshein, Luca Antiga, et al. Pytorch: An imperative style, high-performance deep learning library. In *Advances in neural information processing systems*, pages 8026–8037, 2019.

[8] Trevor Hastie, Robert Tibshirani, and Jerome Friedman. *The elements of statistical learning: data mining, inference, and prediction*. Springer Science & Business Media, 2009.

[9] Rich Caruana and Alexandru Niculescu-Mizil. An empirical comparison of supervised learning algorithms. In *Proceedings of the 23rd international conference on Machine learning*, pages 161–168, 2006.

[10] Sotiris B Kotsiantis, I Zaharakis, and P Pintelas. Supervised machine learning: A review of classification techniques. *Emerging artificial intelligence applications in computer engineering*, 160(1):3–24, 2007.

[11] Geoffrey E Hinton, Simon Osindero, and Yee-Whye Teh. A fast learning algorithm for deep belief nets. *Neural computation*, 18(7):1527–1554, 2006.

[12] Bernhard E Boser, Isabelle M Guyon, and Vladimir N Vapnik. A training algorithm for optimal margin classifiers. In *Proceedings of the fifth annual workshop on Computational learning theory*, pages 144–152, 1992.

[13] Aurélien Géron. *Hands-on machine learning with Scikit-Learn, Keras, and TensorFlow: Concepts, tools, and techniques to build intelligent systems*. O'Reilly Media, 2019.

[14] Stan Franklin and Art Graesser. Is it an agent, or just a program?: A taxonomy for autonomous agents. In *International Workshop on Agent Theories, Architectures, and Languages*, pages 21–35. Springer, 1996.

[15] Michael Wooldridge. *An introduction to multiagent systems*. John Wiley & Sons, 2009.

[16] Jacob Biamonte, Peter Wittek, Nicola Pancotti, Patrick Rebentrost, Nathan Wiebe, and Seth Lloyd. Quantum machine learning. *Nature*, 549(7671):195–202, 2017.

[17] Jeremy Adcock, Euan Allen, Matthew Day, Stefan Frick, Janna Hinchliff, Mack Johnson, Sam Morley-Short, Sam Pallister, Alasdair Price, and Stasja Stanisic. Advances in quantum machine learning. *arXiv preprint arXiv:1512.02900*, 2015.

[18] Ewin Tang. A quantum-inspired classical algorithm for recommendation systems. In *Proceedings of the 51st Annual ACM SIGACT Symposium on Theory of Computing*, pages 217–228, 2019.

[19] Maria Schuld, Ilya Sinayskiy, and Francesco Petruccione. The quest for a quantum neural network. *Quantum Information Processing*, 13(11):2567–2586, 2014.

[20] Yudong Cao, Gian Giacomo Guerreschi, and Alán Aspuru-Guzik. Quantum neuron: an elementary building block for machine learning on quantum computers. *arXiv preprint arXiv:1711.11240*, 2017.

[21] Seth Lloyd, Masoud Mohseni, and Patrick Rebentrost. Quantum principal component analysis. *Nature Physics*, 10(9):631–633, 2014.

[22] Giuseppe Carleo and Matthias Troyer. Solving the quantum many-body problem with artificial neural networks. *Science*, 355(6325):602–606, 2017.

[23] Giacomo Torlai, Guglielmo Mazzola, Juan Carrasquilla, Matthias Troyer, Roger Melko, and Giuseppe Carleo. Neural-network quantum state tomography. *Nature Physics*, 14(5):447–450, 2018.

[24] Alberto Peruzzo, Jarrod McClean, Peter Shadbolt, Man-Hong Yung, Xiao-Qi Zhou, Peter J Love, Alán Aspuru-Guzik, and Jeremy L O'brien. A variational eigenvalue solver on a photonic quantum processor. *Nature communications*, 5:4213, 2014.

[25] Thomas Back. *Evolutionary algorithms in theory and practice: evolution strategies, evolutionary programming, genetic algorithms*. Oxford university press, 1996.

[26] Kenneth De Jong. Evolutionary computation: a unified approach. In *Proceedings of the 2020 Genetic and Evolutionary Computation Conference Companion*, pages 327–342, 2020.

[27] Sean Luke. 1 essentials of metaheuristicsl. 1.

[28] Lothar M Schmitt. Theory of genetic algorithms. *Theoretical Computer Science*, 259(1-2):1–61, 2001.

[29] John Henry Holland et al. *Adaptation in natural and artificial systems: an introductory analysis with applications to biology, control, and artificial intelligence*. MIT press, 1992.

[30] Nathan Wiebe, Christopher Granade, Christopher Ferrie, and David Cory. Quantum hamiltonian learning using imperfect quantum resources. *Physical Review A*, 89(4):042314, 2014.

[31] Eyal Bairey, Itai Arad, and Netanel H Lindner. Learning a local hamiltonian from local measurements. *Physical review letters*, 122(2):020504, 2019.

[32] Burnham KP Anderson DR. Model selection and multimodel inference: a practical information-theoretic approach, 2002.

[33] Jerome Friedman, Trevor Hastie, and Robert Tibshirani. *The elements of statistical learning*, volume 1. Springer series in statistics New York, 2001.

[34] Christopher Granade, Christopher Ferrie, Steven Casagrande, Ian Hincks, Michal Kononenko, Thomas Alexander, and Yuval Sanders. QInfer: Library for statistical inference in quantum information, 2016.

[35] Arpad E Elo. *The rating of chess players, past and present*. Arco Pub., 1978.

[36] FIFA.com. Who we are - news - 2026 fifa world cup™: Fifa council designates bids for final voting by the fifa congress, Jun 2018.

[37] Christof Neumann, Julie Duboscq, Constance Dubuc, Andri Ginting, Ade Maulana Irwan, Muhammad Agil, Anja Widdig, and Antje Engelhardt. Assessing dominance hierarchies: validation and advantages of progressive evaluation with elo-rating. *Animal Behaviour*, 82(4):911–921, 2011.

[38] Lars Magnus Hvattum and Halvard Arntzen. Using elo ratings for match result prediction in association football. *International Journal of forecasting*, 26(3):460–470, 2010.

[39] Robert E Kass and Adrian E Raftery. Bayes factors. *Journal of the american statistical association*, 90(430):773–795, 1995.

[40] Brian Flynn. Mathematical introduction to quantum computation, 2015. Undergraduate thesis.

[41] Quantum model learning agent documentation. https://quantum-model-learning-agent.readthedocs.io/en/latest/, Jan 2021. [Online; accessed 12. Jan. 2021].

[42] Brian Flynn. Quantum model learning agent. https://github.com/flynnbr11/QMLA, 2021.